Remote Sensing Applications: Society and Environment 37 (2025) 101451

Contents lists available at ScienceDirect

Remote Sensing Applications: Society and Environment

journal homepage: www.elsevier.com/locate/rsase

Hedgerow map of Bavaria, Germany, based on orthophotos and convolutional neural networks

Verena Huber-García [a,*], Jennifer Kriese [a], Sarah Asam [a], Mariel Dirscherl [a], Michael Stellmach [b], Johanna Buchner [b], Kristel Kerler [b], Ursula Gessner [a]

[a] *German Aerospace Center e.V. (DLR), German Remote Sensing Data Center (DFD), Münchener Strasse 20, 82234, Wessling, Germany*
[b] *Bayerisches Landesamt für Umwelt (LfU), Ref. 51 Fachgrundlagen Naturschutz, Bgm.-Ulrich-Str. 160, 86179, Augsburg, Germany*

A R T I C L E I N F O

Keywords:
Linear woody vegetation
Biotopes
Aerial images
CNN
DeepLabV3
Small woody features

A B S T R A C T

Hedgerows play a significant role in biodiversity preservation, carbon sequestration, soil stability and the ecological integrity of rural landscapes. Understanding their current condition and future development is therefore crucial for a range of stakeholders such as municipalities, state agencies or environmental organizations. The wall-to-wall mapping and characterization of hedgerows in-situ is, however, very labour-, time- and cost-intensive. This impedes a regular monitoring at adequate intervals. In the Federal State of Bavaria, Germany, the hedgerow biotope mapping is repeated every 20–30 years for each district. State-wide consistent and up-to-date data are hence not available. In this study we present an approach for mapping all hedgerows in Bavaria using orthophotos and deep learning. We used hedgerow polygons of the federal in-situ biotope mapping from 5 focus districts as well as additional manually digitized polygons as training and test data and orthophotos as input in a DeepLabV3 Convolutional Neural Network (CNN). The CNN has a Resnet50 Backbone and was optimized using the Dice loss as cost function. The orthophotos were acquired in 2019–2021. They have a spatial resolution of 20 cm and were fed to the CNN at tiles of 125 × 125 m. The generated hedgerow probability tiles were post-processed through merging and averaging the overlapping tile boarders, shape simplification and filtering. The resulting hedgerow vector data set achieved medium overall accuracies (precision = 0.43, recall = 0.53, F1-score = 0.48). The model generally overestimated the number of hedgerows, and hedgerows were often confused with riparian as well as urban vegetation. Looking at each hedgerow polygon individually, the mapping accuracy varied considerably, with a median F1-score of 0.51 for all detected objects. In addition, we found differences in accuracies among districts in different landscapes. For example, the Hassberge district, a landscape rich of hedgerows, reached a F1-score of 0.61. A comprehensive comparison with the Copernicus High Resolution Layer (HRL) Small Woody Features (SWF) revealed significant differences between the datasets. About 43 % of the hedgerows in our data set were not present in the SWF layer. Especially narrow, elongated vegetated structures are not captured in the SWF product. This highlights the potential to use our state-wide hedgerow map of Bavaria in combination with the SWF dataset, but also by itself, for a range of administrative, statistical and nature conservation applications.

* Corresponding author.
E-mail addresses: verena.hubergarcia@dlr.de (V. Huber-García), jennifer.kriese@dlr.de (J. Kriese), sarah.asam@dlr.de (S. Asam), mariel.dirscherl@dlr.de (M. Dirscherl), michael.stellmach@lfu.bayern.de (M. Stellmach), johanna.buchner@lfu.bayern.de (J. Buchner), kristel.kerler@lfu.bayern.de (K. Kerler), ursula.gessner@dlr.de (U. Gessner).

https://doi.org/10.1016/j.rsase.2025.101451
Received 29 July 2024; Received in revised form 17 December 2024; Accepted 7 January 2025
Available online 10 January 2025

1. Introduction

Hedgerows, tree lines and other linear woody structures are important features that promote biodiversity in many agriculturally dominated landscapes (Graham et al., 2018; Wolton, 2015). They increase the heterogeneity of the landscape and provide habitats for many species. Birds, small mammals, reptiles and amphibians but also insects use them for breeding, foraging food, as shelter from predators or for navigation (Batáry et al., 2010; Bayerisches Landesamt für Umwelt, 2022c; Boissinot et al., 2019; Lecq et al., 2017; Pelletier-Guittier et al., 2020). They also have a positive effect on soil functioning such as the earth worm diversity, the soil microbiome or the amount of dissolved organic carbon stored in the soil (Holden et al., 2019; Sun et al., 2020). Hedgerows and tree lines further provide multifaceted ecosystem services, such as soil stabilisation, water infiltration, or carbon sequestration (Baudry et al., 2000; Dainese et al., 2017; Drexler et al., 2021; Holden et al., 2019). Some studies even indicate agricultural benefits since hedgerows can enhance crop yields through wind protection and support beneficial insects (Garratt et al., 2017; Montgomery et al., 2020; Morandin et al., 2017).

Several European countries have explicitly included hedgerow protection into their Good Agricultural and Environmental Conditions (GAEC) standards programs, acknowledging the importance of hedgerows and promoting their preservation (European Union, 2013). Additionally, hedgerows play an important role in the EU 2030 Biodiversity Strategy (European Commission, 2020) as well as in the Natura 2000 program (European Environment Agency, 2023), both of which aim to promote habitat connectivity across landscapes. Similar to other parts of Europe, hedgerows are a historically important part of the landscape also in Germany. Our study region Bavaria shows a high landscape diversity with a considerable part of small-scale agriculture where hedgerows are most prevalent. The number of hedgerows and linear woody features in Bavaria has, however, declined largely due to the intensification of agriculture. Starting in the 1950s, the so called 'land consolidation act' aimed to consolidate small and fragmented fields to larger ones to improve efficiency and optimize field management (Magel, 2012). As a consequence, hedgerows, small woody features and field strips were removed, which resulted in rather homogenous landscapes. During the 1970s, the Bavarian government started to map ecologically valuable biotopes to gain a state-wide overview and to protect them by law (Bayerisches Landesamt für Umwelt, 2022a). In 1998 the protection of hedgerows outside settlements was finally enshrined in the Bavarian Nature Conservation Law, which states that it is forbidden to remove or impair hedgerows. In addition, eco-schemes are in place in Bavaria to incentivise farmers to maintain and plant hedgerows by compensating extra hardship (Bayerisches Staatsministerium für Ernährung, 2023).

In order to ensure compliance with law and to allocate subsidies correctly, it is important to know the location and extent of hedgerows and to document possible changes. Such monitoring efforts may further be of use for other applications like the estimation of biomass or carbon storage of woody vegetation outside forests (Liu et al., 2023). The Bavarian Environment Agency (LfU) is in charge of carrying out a state-wide biotope mapping in Bavaria. During field campaigns, bushes, hedgerows and woody plants are mapped and subdivided into biotope types based on location, shape, composition and ecological value (Bayerisches Landesamt für Umwelt, 2022b). This task is very time-consuming and labour-intensive and consequently conducted only every 20–30 years for each Bavarian district sequentially. This makes it difficult to track changes over time and to respond in a timely manner. Thus, the LfU, as well as environmental agencies of other federal states, is looking for ways to support the biotope mapping process with additional approaches. During the last years, space and airborne remote sensing data are increasingly used to accurately map the land surface at regular intervals. A remote sensing-based biotope mapping has therefore great potential to support the regular biotope mapping by facilitating the campaign planning, speeding up the mapping process and enabling regular reporting on statistical metrics such as hedgerow loss rates. It can further provide information on biotope connectivity and landscape heterogeneity.

Over the last years, deep learning has gained relevance in many remote sensing applications. This is also reflected in the number of publications on land use and land cover (LULC) classification using deep learning which has considerably increased since 2015 (Digra et al., 2022; Vali et al., 2020; Zhao et al., 2023). Thereby, CNNs (Convolutional Neural Networks) are the most popular architecture for remote sensing applications (Digra et al., 2022; Ma et al., 2019). Deep learning methods were so far mainly used for the detection, classification and segmentation of artificial surfaces and objects (Hoeser et al., 2020). Most publications focus on transportation and settlement while a second group addresses either LULC or agriculture related topics like crop type classification or the mapping of field delineations (Hoeser et al., 2020). There are few recent studies that apply deep learning techniques on remote sensing data to quantify woody vegetation, i.e. Liu et al. (2023) who map trees outside forests across Europe, and Strnad et al. (2023) who detect woody vegetation landscape features for a study region in Slovenia. Kriese et al. (2022) map windbreaks from synthetic data derived from Earth Observation (EO) data in Paraguay, while Brandt et al. (2020) and Tucker et al. (2023) map trees and shrubs outside forests in the African Savanna and Sahel zone by means of deep learning. However, to our knowledge, there is only one publication that applies a neural network to exclusively map hedgerows (Ahlswede et al., 2021). Most publications that use remote sensing data to detect hedgerows either use object-based image analysis (OBIA) (Aksoy et al., 2010; Arias et al., 2013; Betbeder et al., 2014; Burke et al., 2019; Ghimire et al., 2014; Tansey et al., 2009; Vannier and Hubert-Moy, 2008, 2010, 2014) or even conduct their analysis on manually digitized hedgerows (Deng et al. 2013, 2016, 2023; Piwowar et al., 2016). Other methods such as morphological operators (Fauvel et al. 2012, 2014), or random forest classifiers (O'Connell et al., 2015) are also used occasionally.

In addition, most of the publications relying on remote sensing for mapping hedgerows or shelterbelts investigate only small study areas of less than 150 km^2 (Aksoy et al., 2010; Betbeder et al., 2015; Betbeder et al., 2014; Ducrot et al., 2012; O'Connell et al., 2015; Smigaj and Gaulton, 2021; Vannier and Hubert-Moy, 2008, 2010, 2014). Most studies covering large areas of more than 3000 km^2 examine regions with homogeneous landscapes such as Kansas (Ghimire et al., 2014), North Dakota (Burke et al., 2019), parts of the Chinese province Jilin (Deng et al. 2013, 2016), Saskatchewan (Piwowar et al., 2016). Liu et al. (2023) apply a deep learning approach to derive maps of trees outside forests across entire Europe, however not focusing exclusively on hedgerows. And Tucker et al. (2023)

map tree crowns across semi-arid sub-Saharan Africa north of the Equator, however explicitly excluding bushes and separating clumped trees. In fact, the advantages of using neural networks are that taking spatial context into account improves extraction quality, and that no manual feature design is necessary (Ahlswede et al., 2021; Wurm et al., 2019; Oquab et al., 2014). This is particularly beneficial for working with large and geographically heterogeneous study areas, since it increases the transferability of a trained model and therewith model performance. Traditional approaches such as OBIA are limited in terms of their spatial transferability, as expert knowledge and tedious manual feature engineering are required (e.g. Aksoy et al., 2010).

Different EO data are put to use for the mapping of linear woody structures. Most applications rely on optical satellite images (Ahlswede et al., 2021; Aksoy et al., 2010; Arias et al., 2013; Betbeder et al. 2014, 2015; Deng et al. 2013, 2016; Ducrot et al., 2012; Fauvel et al. 2012, 2014; Vannier and Hubert-Moy, 2008, 2010, 2014) or aerial photographs (Burke et al., 2019; Ghimire et al., 2014; O'Connell et al., 2015; Piwowar et al., 2016; Tansey et al., 2009). Betbeder et al. (2014) and Luscombe et al. (2023) include also microwave remote sensing data. Several publications make further use of LiDAR data (Broughton et al., 2024; Luscombe et al., 2023; Strnad et al., 2023; Vannier and Hubert-Moy, 2014). The different data sources cover also a wide range of spatial resolutions. Vannier and Hubert-Moy (2014) compare four different optical satellite sensors with 1–23 m pixel size and panchromatic orthophotos with 0.5 m pixel size. They conclude that the higher the spatial resolution the better the results. However, this only applies under the condition that spectral information beyond a panchromatic channel is available. In the case of Vannier and Hubert-Moy (2014), they achieve the best results with KOMPSAT II having a resolution of 4 m (1 m) in RGB-NIR (panchromatic).

Mapping hedgerows over large areas is a complex task, so only a limited number of countries possess nationwide datasets on their distribution. Nationwide hedgerow datasets exist for the UK (Broughton et al., 2024; Luscombe et al., 2023) and for France as part of

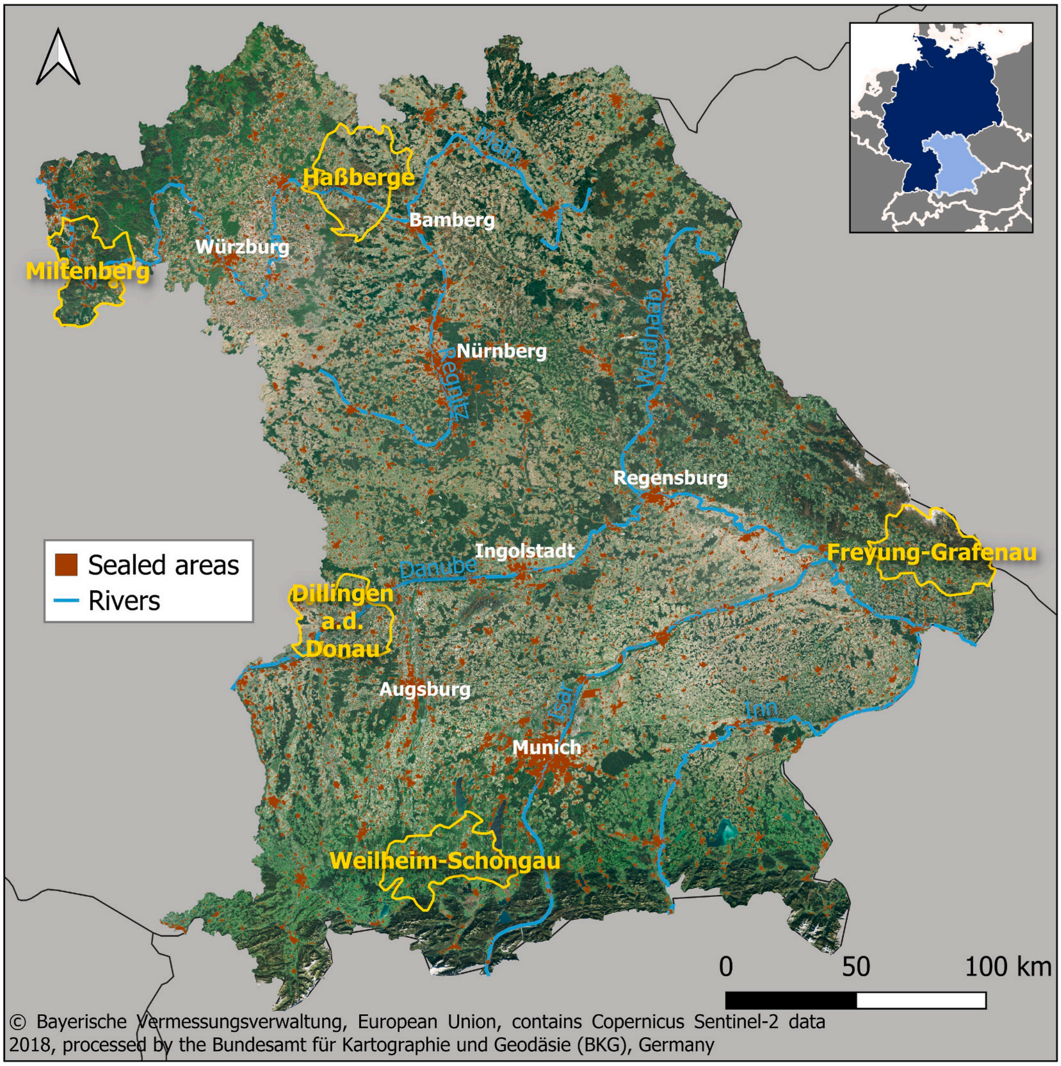

Fig. 1. Overview of the study area, the state of Bavaria in Germany with the five focus districts highlighted in yellow. Sealed areas are derived from CORINE Land Cover 2018; CLMS 2020).

the BD TOPO® vector dataset (Institut National de l'Information Géoraphique et Forestière, 2021), while for Germany, the only EO based dataset available so far that includes hedgerows is the high-resolution Small Woody Features (SWF) layer published by the European Union's Copernicus Land Monitoring Service (CLMS) (CLMS, 2019, 2023). This dataset contains various SWF, defined as "linear or patchy structures of woody/scrubby/bushy vegetation" (CLMS, 2021). Hedgerows are thus included as feature type, but the dataset does not exclusively differentiate them. It is produced using geographic object-based image analysis (GEOBIA) that relies on two main components: i) feature extraction derived from attribute profiles and ii) a semi-supervised classification based on a random forest algorithm (CLMS, 2021). The main data source for the SWF 2018 layer is the VHR_IMAGE_2018 dataset provided by the European Space Agency (ESA) Copernicus Space Component Data Access (CSCDA) (CLMS, 2021). This EO dataset comprises very high-resolution data from several satellite missions delivered at 2–4 m spatial resolution and for four spectral bands (blue, green, red and NIR).

To provide comprehensive information on the current state-wide distribution of hedgerows, our goal was to develop an approach to derive hedgerows for the whole state of Bavaria from EO data by means of deep learning. The intention was to use data freely available to many public authorities within Germany to allow for repeatability and spatial transferability, as well as to facilitate the user uptake. Thus, we used aerial imagery with 20 cm resolution in combination with in-situ biotope mapping data gathered by the federal environmental agency. We further assessed the potential of this approach to support mapping tasks by providing an automated and reproducible procedure for mapping hedgerows. Our objectives were to create a wall-to-wall hedgerow map for Bavaria and to discuss its suitability to e.g., support in-situ biotope mapping of hedgerows by public agencies but also its potential to serve other uses such as carbon storage and biomass assessments or studies on landscape heterogeneity. Further, differences and similarities to the Copernicus SWF layer and to the canopy cover map by Liu et al. (2023) were analysed. More specifically, this study addressed the following questions.

- At what accuracy is a deep learning model in combination with aerial imagery and in-situ reference data able to detect hedgerows across the study region with a high landscape diversity?
- Which implications does the use of a single trained model have on a state-wide hedgerow detection in a heterogeneous landscape?
- How does the deep-learning based hedgerow mapping compare to other datasets such as SWF or the canopy cover map by Liu et al. (2023)? Does it provide additional information?
- How can the automated hedgerow detection be of use for the mapping of biotopes and other biotope related applications? What limitations and opportunities exist?

2. Study area and materials

2.1. Study area

Fig. 1 shows the study area of Bavaria, which is the largest federal German state covering 70,550 km^2, located in the Southeast of the country. Around 35% of the area is covered by forests and 46% are used for agriculture (Bayerisches Landesamt für Statistik 2023a, b), of which approx. 1/3 is permanent grasslands (Bayerisches Landesamt für Statistik, 2023a). To capture the landscape diversity present in Bavaria, we selected five focus districts (Fig. 1 and Table 1) that are spread across the state and for which recent in-situ biotope data are available.

2.2. Reference data

For our automatic hedgerow mapping, we used a supervised learning method which required reference information on the exact location and extent of all hedgerows. These are provided by in-situ mapped polygons that LfU recorded during their biotope mapping campaigns in the districts Freyung-Grafenau, Miltenberg, Hassberge, Dillingen and Weilheim-Schongau from 2018 to 2020 (see Fig. 1). Biotopes are mapped in the field by drawing them on topographic maps and are digitized on an aerial image later. Further characteristics such as species composition, biotope type and impairments are additionally recorded in-situ following a strict protocol (Bayerisches Landesamt für Umwelt, 2022a). The biotope type is selected from a list providing 80 different types. Nine of these biotope types are listed under the category 'shrubbery, hedgerows, woody plants' with natural hedgerows being one of them. They mainly grow along agricultural fields, smaller roads and embankments, are structurally rich and dominated by former human use and management. The species composition of natural hedgerows consists of native plants and further criteria such as age determine their ecological value. Hence, hedgerows dominated by needleleaf species or neophytes, hedgerows younger than 10 years or those with missing undergrowth are not mapped as hedgerow biotopes in the field (Bayerisches Landesamt für Umwelt, 2022b). Further, the in-situ mapped biotopes can represent a biotope complex, including multiple biotope types within one complex. The amount of a biotope type within each complex is given by a percentage value. For our focus districts, we selected all biotopes of the type 'natural hedgerow' with a minimum share of 90% within a complex, collected between 2018 and 2020 (3200 in total). This in turn means that we excluded complexes with a lower proportion because the exact location of the hedgerow is unknown.

The definition of hedgerows in the in-situ biotope mapping protocol (Bayerisches Landesamt für Umwelt, 2022b) concentrates on hedgerow age, the condition of the understory or species composition. It usually does not contain linear woody vegetation along watercourses, as these features are mainly categorized as the biotope type "riparian vegetation". Still, depending on the dominant species it may be categorized as hedgerow. The case for hedgerows accompanying roads is similar: They are often, but not always, poor in species diversity and therefore not mapped as biotopes. According to the protocol, hedgerows are linear woody structures which are

Table 1
Characteristics of the five focus districts. Precipitation data is the multiannual mean of 1991–2020 derived from the HYRAS data set of DWD (Razafimaharo et al., 2020). Percentages on biotope area are obtained from the biotope mapping provided by the Bavarian Environment Agency (Bayerisches Landesamt für Umwelt, 2024).

Focus district	Location in Bavaria	Altitudinal range [m a.s.l.]	Mean yearly Precip.	Landscape	Biotope area share	Of these: Hedgerow biotopes	Other common biotopes
Miltenberg	North-West: Odenwald, Spessart	100–600 m	778 mm	Small-scale cropping, vineyards	4 %	10 %	Other woody biotopes: orchards, bushes, field copses, trees/shrubs along watercourses
Hassberge	North, southwestern German stratified plateau	200–500 m	699 mm	Small-scale landscape and substantial forest cover in some areas	4 %	10%	Other woody biotopes as well as extensively managed grasslands
Dillingen a.d. Donau	West, Donauried with Iller-Lech Plateau to the South and Swabian Jura to the North	400–650 m	746 mm	Intensive use of cropland	2 %	5 %	Wet meadows and other wetland and water biotopes
Freyung-Grafenau	East, Bavarian Forest	300–1500 m	1162 mm	Rolling hills, small-scale grassland farming	5 %	10 %	Wetland biotopes: Wet meadows, Bristlegrass turf
Weilheim-Schongau	South, Alpine foreland	530–1600 m	1184 mm	Dominated by grassland farming	10 %	1 %	Peatland and other wetland biotopes

up to approx. 10 m wide, but further information on geometrical features that could be distinguished from orthophotos is not provided. Hence, we expected that most of the characteristics that distinguish a biotope hedgerow from a hedgerow of less ecological value or other hedgerow-like structures cannot be identified spectrally and/or geometrically on orthophotos. This hypothesis was supported by tests which revealed that leaving out hedgerows of less ecological value from the training would confuse the learning process of the model and eventually lead to less accurate results. As a consequence, we built a training and validation dataset that included both biotope hedgerows and hedgerows of less ecological value that have similar morphological characteristics. These characteristics were defined as follows: The features are linear woody structures made up of bushes and/or trees without any gaps. Their average width is below 10 m and they cover an area of at least 70 m^2. We digitized manually another 4356 hedgerow polygons based on aerial images following these rules. Linear structures along watercourses were not digitized, as they belong for the largest part to the biotope class “riparian vegetation”, its allowed max. width being 20 m and therefore considerably wider than the one of hedgerows. Linear woody features along roads were not added as they usually are not included in the biotope mapping. The additional digitalization was carried out in all five focus districts. We checked the statistical distribution of area, length and width values for biotope hedgerows and manually digitized hedgerows to make sure they agree well. Different experts digitized the additional hedgerows independently for the test dataset to ensure unbiased test samples for the accuracy assessment (Maxwell et al., 2021). These additionally digitized hedgerows are called ‘additional hedgerows’ hereafter, the biotope hedgerows are called ‘natural hedgerows’. Together, the 3200 natural and 4356 additional hedgerows constitute the ground truth reference data. This dataset was further split in training, validation and test dataset in the same way as the corresponding orthophotos, see section 3.1.

2.3. Remote sensing data

We used orthorectified aerial RGB images to automatically map hedgerows. The images with a spatial resolution of 20 cm were acquired over an approximately two-year period by the Bavarian Agency for Digitalization, High-Speed Internet and Surveying. Due to the approx. bi-yearly acquisition, this dataset is well suited for the repeated mapping of hedgerows by means of remote sensing. Changes over time could be monitored at a bi-yearly cycle, hence providing additional information to the mapping carried out by the LfU every 20–30 years. The images were acquired in the years 2019, 2020 and 2021 between April and September, respectively. Our final dataset included a total of 18,647 images, with a size of 2 km × 2 km each, covering the whole state of Bavaria. The very high spatial resolution of 20 cm allowed the CNN to take into account both the shape and texture as well as the spatial context, while learning how to detect hedgerows. We used RGB spectral bands, because former analyses in our study region have shown that observations in the near-infrared domain do not improve the mapping of hedgerows substantially (Ahlswede et al., 2021).

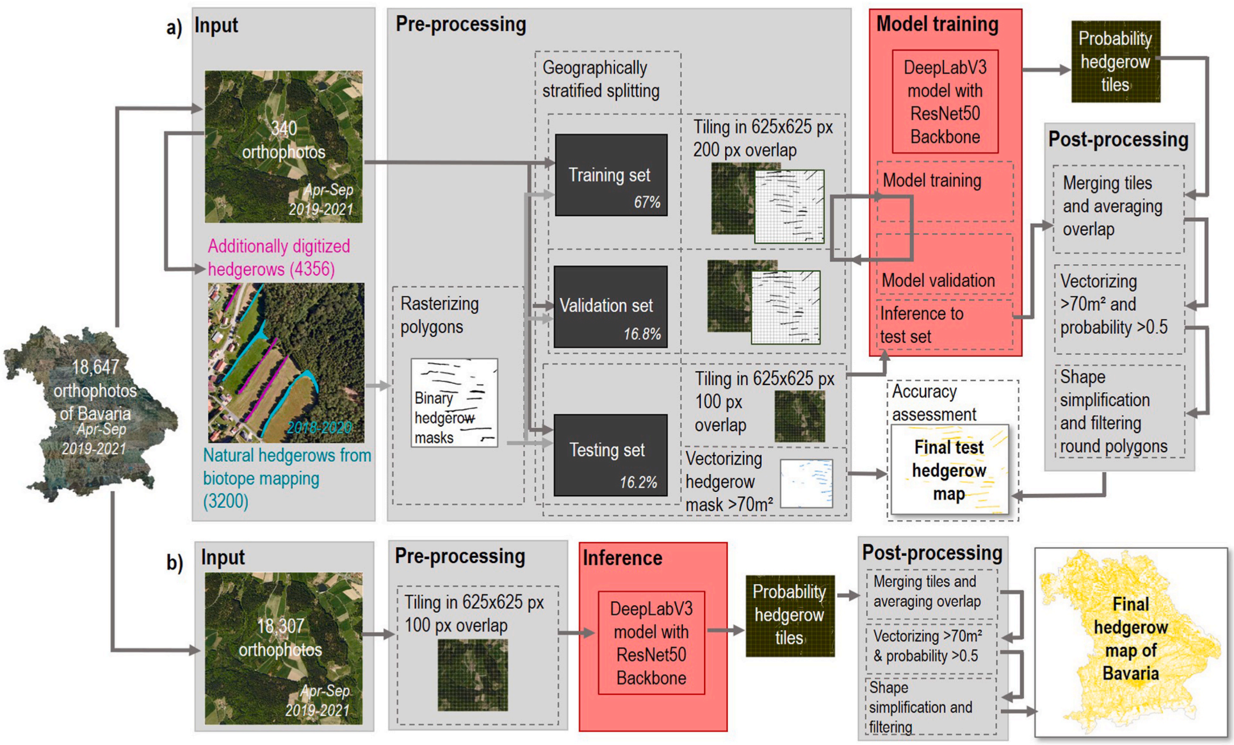

Fig. 2. Workflow for automated hedgerow mapping using a CNN and orthophotos including a) the training and testing in five focus regions and b) the inference of the model to the whole of Bavaria.

2.4. Copernicus HRL Small Woody Features

The pan-European high-resolution layer (HRL) SWF 2018 (https://doi.org/10.2909/7fd9d32e-8c2f-42b2-b959-c8e12b843821) published by the CLMS (2023) was used for a descriptive comparison with the mapping results of this study. The SWF dataset is produced using a combination of GEOBIA and random-forest classification on VHR spaceborne remote sensing data with a spatial resolution of 2–4 m (CLMS, 2021). The final product has a resolution of 5 m and is also available as vector layer (CLMS, 2021). To date, SWF layers have been released for the reference years 2015 and 2018 (CLMS, 2019, 2023). The 2018 layer, derived from satellite imagery captured in 2017, 2018, and 2019, was used in this study because its temporal coverage aligns best with the in-situ and remote sensing data employed for our automated hedgerow mapping. The exact acquisition dates for Bavaria are unknown, but the maximum time gap between the SWF data and our orthophotos is estimated to be up to 4 years.

2.5. Canopy cover map

We further compared our dataset to the tree map published by Liu et al. (2023). They trained a CNN with airborne LiDAR data to produce a binary canopy cover map and to predict tree height from PlanetScope imagery for the year 2019. The final dataset provides information on the location and canopy height of trees at a 3 m resolution across all Europe. While the dataset does not specifically focus on hedgerows, it encompasses all vegetation outside forests taller than 3 m. As a result, there might be a significant overlap with our hedgerow map.

3. Methods

The automated mapping of hedgerows included several processing steps (Fig. 2 a). In a first step, hedgerows and the digitalization of additional hedgerow polygons, see section 2.2. Second, we transformed all reference hedgerow polygons into rasterized binary hedgerow masks based on the 20 cm pixel grid of the orthoimages. In a next step, these masks were tiled and split into a training, validation and test region, in the same way as the orthophotos. These pre-processing steps are described in more detail in section 3.1. The training and validation sets were passed to a CNN model which learned to detect hedgerows from the tiled orthophotos in an iterative process (section 3.2). Eventually, the model predicted a probability hedgerow map for each tile. In a final step, we merged and vectorized the tiles and applied further post-processing to the segmented hedgerow polygons (section 3.3) before finally assessing the accuracy of the model results with respect to the part of the reference dataset that was aside for testing (section 3.4). In a last step, all orthophotos as well as the trained model and post-processing procedure were used to infer the mapping to the whole of Bavaria (Fig. 2 b).

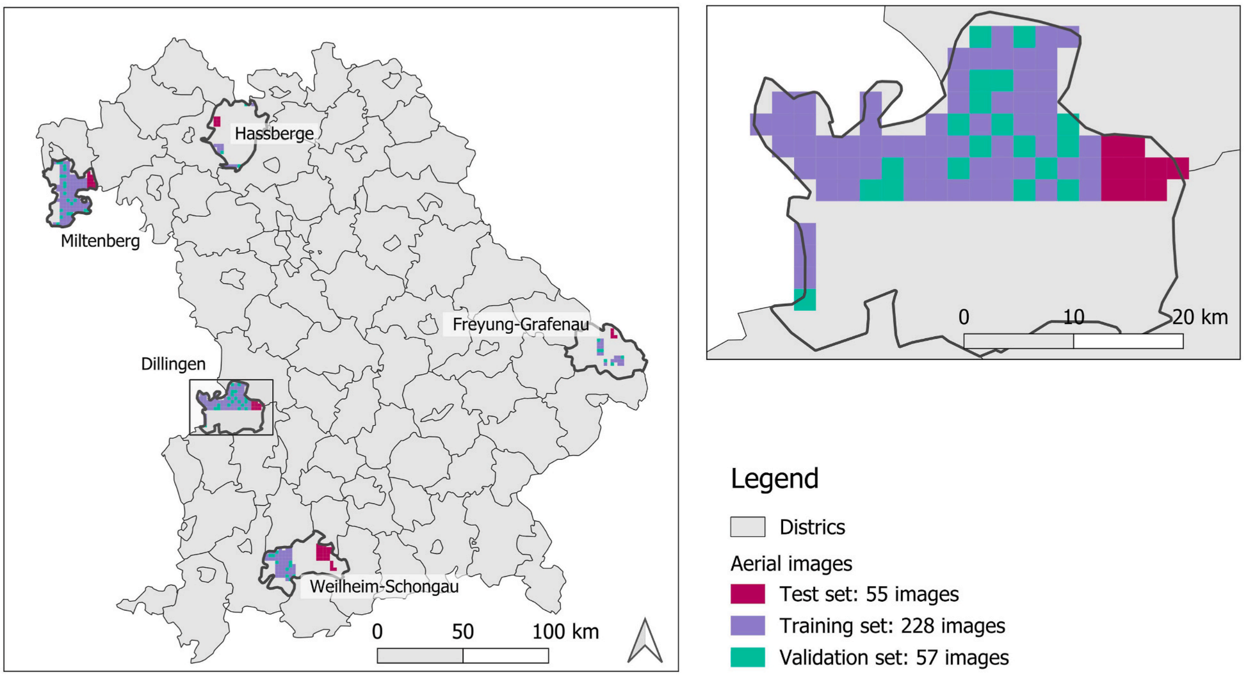

Fig. 3. Spatial distribution of aerial images of Bavaria used for training, validation and testing (left) and close-up of the Dillingen district that exemplarily shows the dataset splitting applied to the aerial images (right).

3.1. Selection and tiling of orthophotos

To guarantee a meaningful accuracy assessment, we selected the orthophotos for testing based on geographically stratified partitioning (Maxwell et al., 2021). This sampling method reduces the spatial autocorrelation between the data subsets (Maxwell et al., 2021). The remaining dataset was split for training and validation using a tessellation stratified random chip partitioning (Maxwell et al., 2021). In this way, similar hedgerow proportions in the training and validation sets were achieved. We only selected those orthophotos and corresponding reference polygons within our focus regions whose areas were entirely mapped during the biotope mapping campaigns 2018–2020, resulting in 340 aerial images. The final training set comprised 228 orthophotos (67%), the validation set 57 (16.8%) and the test set 55 (16.2%), distributed over the districts Freyung-Grafenau (training & validation: 22/test: 4), Miltenberg (112/11), Hassberge (14/6), Dillingen (80/9) and Weilheim-Schongau (57/25) (see the distribution over Bavaria in Fig. 3). Finally, we transformed the reference polygons into a binary hedgerow mask and split accordingly.

We used a single Geforce RTX 2080 Ti GPU with 11 GB of memory for processing, which forced us to balance the number of model parameters and the size (number of pixels) of the input images. In this respect, we had to consider whether a finer spatial resolution is of higher importance than a spatially larger image extent with lower resolution including more spatial context around the hedgerows. We carried out several tests with varying pixel and image tile sizes which showed that using the original high resolution of 20 cm and a tile size of 125 × 125 m led to better results than using image tiles with a larger spatial extent of 500 × 500 m but a lower resolution of 40 cm. In order to train the CNN model, we eventually cropped each orthophoto (original dimensions: 3x10,000x10,000 pixels) and the corresponding binary hedgerow masks into 361 tiles of 3x625x625 pixels with a spatial overlap of 200 pixels (i.e. 40 m) between neighbouring tiles. The overlap of 200 pixels was selected to ensure that hedgerows cropped at the image borders are present at their entire length at least in one of the image tiles. This is important because classification quality near the image border is lower (Maxwell et al., 2021) and cropped hedgerows are more difficult to identify. Following the approach of Ahlswede et al. (2021), out of these image tiles, only those containing hedgerows were used for training and validation. Hence, the dataset eventually contained 13,142 tiles in the training set and 3732 tiles in the validation set. In contrast, the aerial images of the test set were cropped with an overlap of only 100 pixels to reduce the time for tiling, inference and merging. All image tiles, i.e. also those containing no hedgerows, were kept in the test set which hence comprised 19,855 tiles. As for the application to the whole of Bavaria, the remaining 18,307 orthophotos were tiled like the test set with an overlap of 100 pixels and passed to the model.

3.2. Model architecture

The CNN model architecture we used in this study for the segmentation of hedgerows is a DeepLabV3 with a ResNet50 backbone (Chen et al., 2017). DeepLabV3 consists of an encoder, which is the model's backbone extracting feature information, and a decoder. The decoder reconstructs the spatial composition of the image and transforms the feature information into pixel-level classifications. The atrous spatial pyramid pooling (ASPP) module in the decoder allows using different dilation rates in parallel to increase the filter's field of view and learns to reconstruct spatial features on multiple scales. This is advantageous, because the spatial resolution is kept while different dilation rates enable to extract features at different fields of view (multiscale features). Hence, it enables a better consideration of the spatial image context, e.g., for the segmentation of image objects with strongly varying sizes such as hedgerows (Dirscherl et al., 2021). Further, it supports the attention to detail and results in less blobby segmentation results (Dirscherl et al., 2021). The module in the used model layout has four parallel convolutional layers: one 1x1 convolution and three 3x3 convolutions with dilation rates of 12, 24, 36 and an average pooling in the end. The final layer of the decoder has a depth of two and is derived through a 1x1 convolution followed by a sigmoid activation function. The two resulting segmentation masks provide the classification for the pixels to belong to the class 'hedgerow' or 'background'.

The DeepLabV3 with the ResNet50 backbone keeps a residual connection between the input layer and the output of the convolution. This kind of architecture maintains detail in the convoluted data and therefore constructs deeper models which perform better (Dirscherl et al., 2021; He et al., 2016). We used the PyTorch model implementation which had initially been trained on a subset of the Common Objects in Context (COCO) dataset, containing 20 different classes (Torch Contibutors, 2023). The pretrained weights were used as initialization but all 41,999,191 parameters were optimized during training.

The cost function is provided by the Dice loss (DL) (shuaizzZ, 2020) as provided in eq. 1 which quantifies the agreement between the predicted class probability p_i and the ground truth label g_i (Zhao et al., 2020). This measure is particularly suitable for imbalanced segmentation tasks such as boundary detection or mapping of rare objects (Zhao et al., 2020).

$$DL = 1 - \frac{2\sum_{i=1}^{N} p_i g_i}{\sum_{i=1}^{N} p_i^2 + \sum_{i=1}^{N} g_i^2} \quad (1)$$

To optimize the loss function, we used the Adam optimizer (Kingma and Lei Ba, 2015) with a maximum learning rate of 5e-5. If there was no improvement in reducing the validation loss for three epochs, the training was automatically terminated.

For model training, we used 13,142 training and 3732 validation sample tiles (as described in section 3.1) which were parsed in batches of three. All samples were normalized and a random horizontal flip was applied as on the fly data augmentation. Further geometric augmentation was not applied since too strong or "wrong" augmentation can introduce systematics to the data that do not occur in the original images (Ahlswede et al., 2021). Besides, we considered the training and validation set comprising in total almost 17,000 samples to be large enough and sufficient without strong augmentation. We did not apply any radiometric augmentation because all aerial images used for training, testing and for the subsequent Bavaria-wide hedgerow mapping were acquired by the same sensor. Moreover, the in-detail analysis of Ahlswede et al. (2021) has revealed, that the use of radiometric and geometric augmentation leads to less accurate predictions compared to a purely geometric augmentation. Eventually, the we applied the trained model to the test dataset and obtained hedgerow probability tiles.

3.3. Post-processing

To derive a final binary classification from the hedgerow probability tiles, we merged all tiles that belonged to one orthophoto. In areas where neighbouring tiles overlap we calculated the average probability of all overlapping tiles per pixel. In this way, the overlap of tiles by 200 pixels for the training and validation regions and 100 pixels for the test region and inference to the rest of Bavaria reduces misclassifications at tile borders in the final mapping result. Subsequently, all pixels with a probability equal to or higher than 0.5 were selected and vectorized obtaining hedgerow polygons. Further, polygons smaller than 70 m^2 were discarded as it was obvious from the used field data, that hardly any hedgerows in our study region were smaller than this size. In addition, round polygons were omitted, as hedgerows occur in elongated shapes by definition. For this purpose, we simplified every hedgerow polygon with the Visvalingam algorithm (Visvalingam and Whyatt, 1993) with a tolerance of 1 m in QGIS. For each of the simplified polygons the shape index *SI* (eq. (2)) was calculated which describes the shape of a polygon independently of its size (McGarigal, 2015) and hedgerows with $SI < 1.6$ were excluded. This value was chosen as 95% of the used in-situ hedgerows have an SI above 1.6.

$$SI = \frac{0.25 * perimeter}{\sqrt{area}} \tag{2}$$

In order to make the classification results comparable to the reference data, the SI was also applied to the reference hedgerow polygons of the test dataset before evaluating the post-processed segmentation results.

3.4. Evaluation

For the evaluation of the model, we calculated the precision (P), recall (R) and F1-score, see eqs. (3)–(5) using true positive (TP), false positive (FP) and false negative (FN) predictions:

$$P = \frac{TP}{TP + FP} \tag{3}$$

$$R = \frac{TP}{TP + FN} \tag{4}$$

$$F1 - Score = 2 * \frac{\dot{P} * R}{P + R} \tag{5}$$

For the sake of clarity, we refer to the natural and additional hedgerows in the test dataset as “ground truth hedgerow polygons” and the hedgerows that were detected by the deep learning model, as “classified hedgerow polygons” hereafter. The evaluation metrics were calculated both at pixel level, i.e. comparing the total overlapping and non-overlapping areas of classified and ground truth hedgerow polygons, and for each ground truth hedgerow polygon individually.

4. Results

4.1. Classification accuracies

The evaluation metrics of the hedgerow classification are summarized in Table 2. For the entire test dataset considering all five focus districts the trained model achieved a precision of 0.43. This means that 43% of the area classified as hedgerow was actually ground truth hedgerow area. In turn, the value indicates that 57% of the area classified as hedgerow was not covered by ground truth

Table 2
Evaluation results at pixel level for the entire test set and for each of the five focus districts individually.

	Precision	Recall	F1-Score
Entire test set	**0.43**	**0.53**	**0.48**
Miltenberg	0.33	0.47	0.39
Weilheim-Schongau	0.41	0.48	0.44
Dillingen	0.52	0.48	0.50
Freyung-Grafenau	0.45	0.76	0.57
Hassberge	0.55	0.68	0.61

hedgerow polygons. The recall at pixel level is 0.53, i.e. 53% of the area of ground truth hedgerow polygons was actually mapped as hedgerow. As for the F1-score, which represents the harmonic mean between precision and recall, the trained CNN achieved 0.48.

The evaluation metrics at pixel level were also calculated for each of the five focus districts individually, see Table 2. The accuracy of the hedgerow mapping varied considerably among districts. Both precision and recall were lowest for Miltenberg, followed by Weilheim-Schongau. For these two districts, accuracy metrics were below the ones for the entire test set, see Table 2. The best accuracies were achieved in Freyung-Grafenau for the recall, where 76% of the ground truth hedgerow area was correctly detected, and in Hassberge for the precision. In this district, 55% of the classified hedgerow area coincided with the ground truth hedgerow area. The F1-score of 0.61 for Hassberge was the highest at district level.

The distribution of precision, recall and F1-Score calculated for each ground truth hedgerow polygon individually is displayed in Fig. 4. The median precision was 0.48, the median recall 0.64 and the median F1-Score reached 0.51. The values at individual polygon level were hence slightly higher as at pixel level. Fig. 4 shows the wide range of values that the precision, recall and F1-Score covered when calculating the evaluation metrics at polygon level.

4.2. Mapping results for Bavaria

In total, the derived hedgerow map includes 564,339 polygons after post-processing which add up to an area of 473 km^2. The median area and length are 594 m^2 and 185 m, respectively.

The percentage coverage of hedgerows per km^2 across Bavaria (Fig. 5) shows that hedge densities are generally lower in the South compared to North and East. In the southern part, large areas show percentage coverages below 0.5% or even below 0.25%. These landscapes are often dominated by intensive agriculture (managed grasslands and arable farming), especially in the southern Danube basin (Fig. 1). The metropolitan area of Munich constitutes an exception, see subset B of Fig. 5, showing a close-up of the city of Munich, where most pixels reach values between 1% and 4%. The location of rivers such as the Isar, Inn or Danube (see Fig. 1) can be identified as regions of high hedgerow density in the south (Fig. 5) indicating the presence of riparian vegetation. North of the Danube river the occurrence of hedgerows is generally higher according to the mapping results. Here, landscapes are more finely structured due to a more small-scaled relief with many hills and small rivers. In the mountainous regions on the southern border of Bavaria, however, hedgerows are nearly inexistent. The areas with almost no hedgerow coverage in the very South coincide with mountain forests on steep slopes or bed rock. Also, other areas across Bavaria where hedgerows do not occur (white patches in Fig. 5) are dominated by large cohesive forests or lakes.

Subsets A and C of Fig. 5 provide a more detailed view of the areas with highest hedgerow coverages per km^2. In the municipality of Bischofsheim in der Rhön (subset A), the hedgerow area adds up to 8.75% per km^2, the overall highest value. The classified hedgerow polygons displayed in grey in subset A confirm the high density of hedgerows in this area lying close together and mostly running in parallel. Another hedgerow hotspot with similar parallel patterns is the Isar valley close to Gaissach in subset C (see also Fig. 11 c)). Here, the hedgerow coverage per km^2 reaches a maximum of 6.58%. Subset B shows parts of the English Garden in Munich, an extensive park, which reaches values of up to 3.90%.

Also at municipal level (*Gemeinde*, Local administrative unit (LAU) 2) the spatial distribution of hedgerows is not homogeneous across Bavaria (Fig. 6). Ten out of eleven municipalities with coverage values above 2% are located in the northern and eastern part of Bavaria. The only exception is Unterföhring (2.63%), NE of the city of Munich, which is the municipality with the overall highest hedgerow percentages. Urban areas show generally higher hedgerow percentages. Out of the ten largest Bavarian cities, six reach values above 1% (Munich 1.64%, Nuremberg 1.10%, Regensburg 1.36%, Fürth 1.40%, Würzburg 1.44%, Erlangen 1.10%) and four above 0.7% (Augsburg 0.78%, Ingolstadt 0.87%, Bamberg 0.85%, Landshut 0.75%), which is above the overall median of 0.64%.

4.3. Detailed mapping evaluation

In the following, typical examples of hedgerows detected with high accuracies (Fig. 7), as well as typical errors (Fig. 8) are

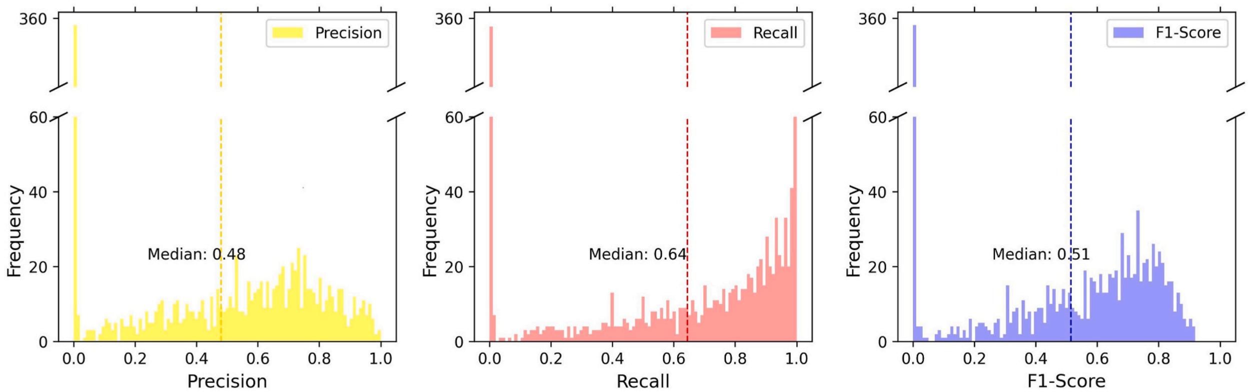

Fig. 4. Distribution of precision, recall and F1-Score calculated for each ground truth hedgerow polygon individually.

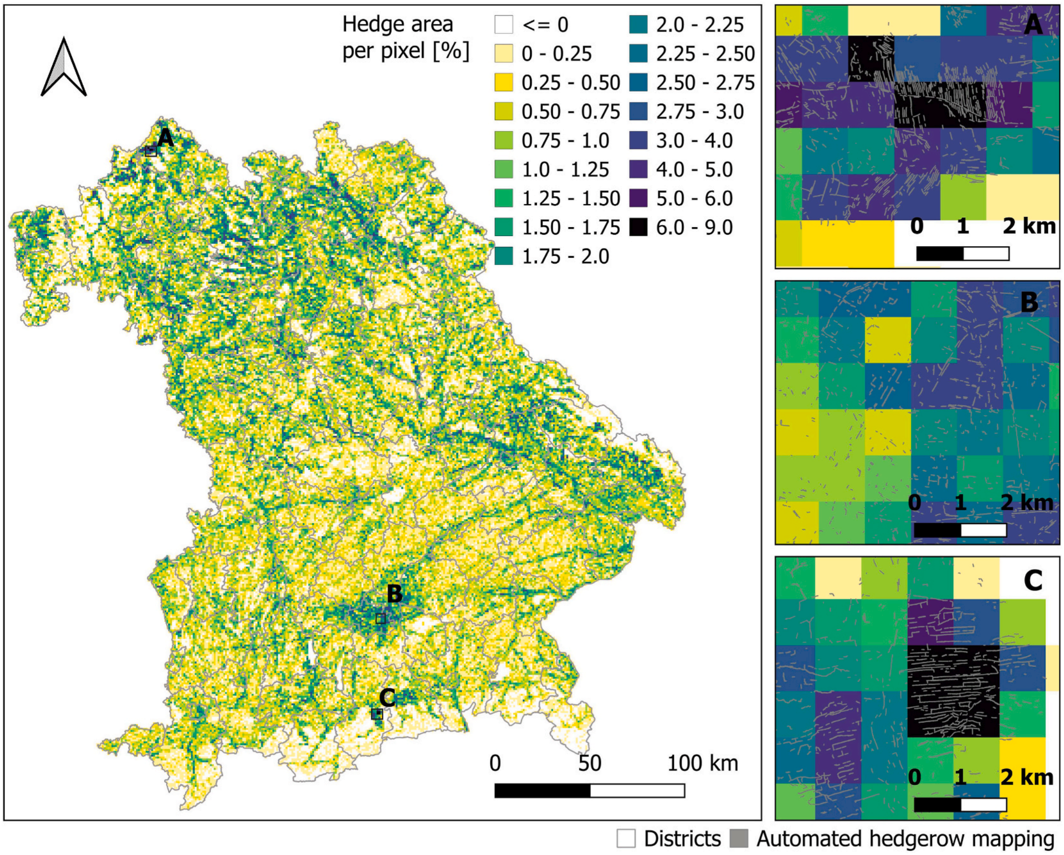

Fig. 5. Hedgerow area per 1 km × 1 km pixel in percent in Bavaria according to the automated mapping overlaid by the classified hedgerow polygons (grey) for three close-ups. Subset A shows a close-up of the municipality Bischofsheim in der Rhön, subset B of Munich including the English Garden and subset C the Isar valley at Gaissach.

illustrated. In the left columns, mapping results for the test regions are shown (a), c) and e)). The right columns (b), d) and f)) show examples of the inference of the model to the whole of Bavaria.

The visual inspection of many examples from different Bavarian landscapes suggests that the trained CNN is capable of nicely identifying and delineating hedgerows and hedgerow-like structures in small-scale structured landscapes also outside the test regions. They are overall well distinguished from similar landscape elements such as copses, orchards or single trees. Hedgerows that are well identifiable by human eyes in the aerial image are usually also well detected by the deep learning model, see Fig. 7.

In Fig. 7 a), each of the parallel hedgerows is properly detected. FN (red) are very few, which leads to a very high recall of 0.95 for this subset. FP detections (blue) occur, because classified hedgerow polygons are often longer and thicker in this example than the ground truth hedgerow polygons. While the model sticks to the exact extent of hedgerow crowns visible from the orthophoto, the shape of the ground truth hedgerow polygons is often smaller, as according to the biotope mapping rules they have to delineate the foot of the hedgerows (Bayerisches Landesamt für Umwelt, 2022b). Besides, they seem to be simplified as they were obtained by manual digitalization. As a consequence, the FP areas sum up to a considerable amount producing only a medium precision of 0.52 and thus a F1-Score of 0.67.

The presented approach is also able to correctly classify rather complex hedgerow structures (Fig. 7 c) and e)). The northern most hedgerow in Fig. 7 c) is detected as a single polygon, showing that the trained CNN is capable of capturing complex hedgerow shapes as continuous objects. The FN (red) are single trees that were not recognized by the model as hedgerow. These missed detections are responsible for the lower recall value of 0.82 as compared to Fig. 7 a). The FP are woody vegetation structures that were not part of the ground truth hedgerow polygons. The precision is still higher as in Fig. 7 a) as the shape mismatch between ground truth and classified hedgerow polygons is less pronounced. Also in Fig. 7 e), the model detects the largest parts of the hedgerows, while tree rows are excluded. Differences between detection result and ground truth occur along polygon edges where the model either classifies a hedgerow broader or longer than the ground truth hedgerow polygon (FP, blue) or misses parts of it (FN, red). Besides, also entire ground truth hedgerow polygons may be missed by the model. In the example in Fig. 7 e) this applies to hedgerows in the south-western part of the subset with very small width. The recall is therefore 0.6, the precision 0.65 and the F1-Score 0.62.

The model distinguishes properly between linear woody vegetation classified as hedgerow and patchy structures or copses also in complex landscapes outside of the focus districts (Fig. 7 b). Besides, linear structures exceeding a certain width are not detected. The

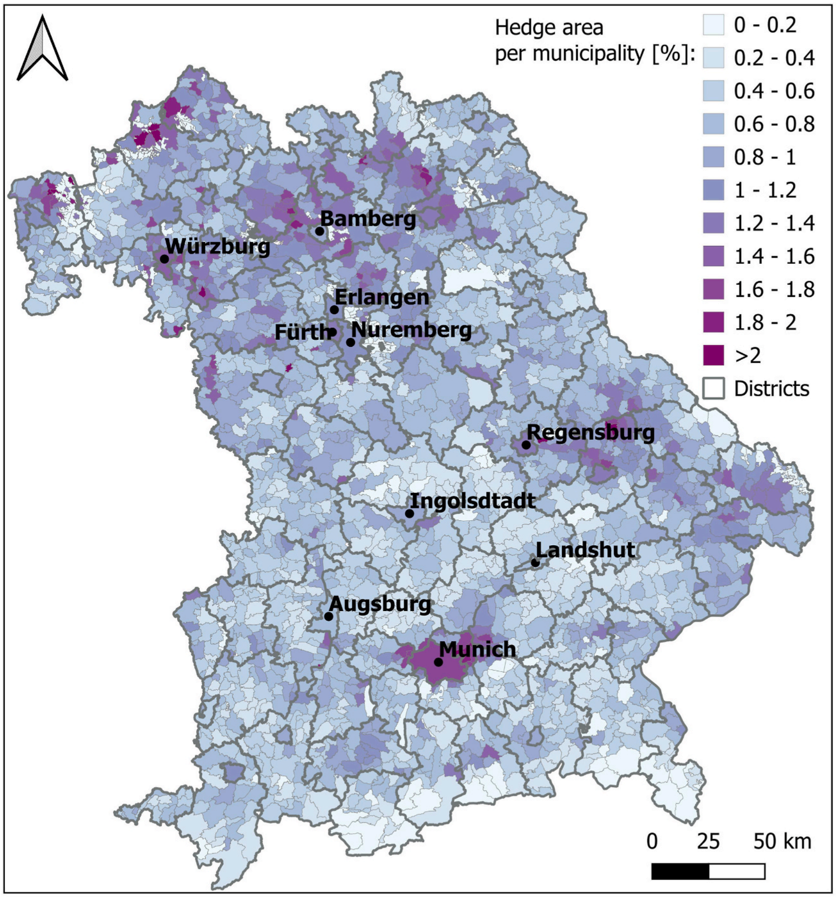

Fig. 6. Overview of percentage area covered by hedgerows at municipality level (Gemeinde, Local administrative unit (LAU) 2) according to the automated hedgerow mapping results for the whole of Bavaria.

hedgerow with the peculiar shape in Fig. 7 d) is also recognized as such, while wider woody structures and single trees in the center of the image are correctly dismissed. Fig. 7 f) illustrates another example where narrow linear woody structures and thicker ones, i.e. copses, coexist in a small area also with an orchard in the lower right corner where trees are planted in rows. As intended, only the narrow linear vegetation structures are mapped as hedgerows.

We also detected some typical classification errors when comparing the classified to the ground truth hedgerow polygons in the test regions. Fig. 8 a) is an example of a false negative prediction: The vertical red polygon to the right is not detected by the model, but was classified during the biotope mapping campaigns as natural hedgerow biotope and is therefore one of the ground truth hedgerow polygons. On the orthophoto used as input to this study, however, no hedgerow is visible at this location. This means that the hedgerow was either coppiced or removed completely at the time of image acquisition. The same ist true for the red curved polygon further to the left. Consequently, the recall is very low (0.17). Meanwhile, the precision is very high (0.97) since FP areas are close to absent. Nevertheless, the final F1-Score for this subset is only 0.29.

Fig. 8 c) shows a case of FP where riparian vegetation was classified as hedgerow by the deep learning model, while it is not part of the ground truth hedgerow polygons causing the precision to reach only 0.24 and the F1-Score 0.36. When inspecting the detection results for all of Bavaria, it becomes clear that the misclassification of riparian vegetation is a typical source of error. Fig. 8 b) shows an example of the municipality of Straubing where woody vegetation along the Danube river and an old meander was labeled as hedgerows by the model. This explains also the higher hedgerow coverage along rivers visible in Fig. 5.

An area in the district of Miltenberg exemplifies the mixed use of land as meadows, cropland, and orchards typical for this region (Fig. 8 e)). This landscape posed a challenge to the deep learning approach resulting in either falsely positive (blue) or falsely negative (red) misclassification. The F1-Score for this subset is consequently only 0.3. Already the digitalization of additional training hedgerows (section 2.2) was challenging in this area. Based on the orthophoto alone it was difficult to decide in this region where to draw the line between a hedgerow and other woody vegetation structures.

Further sources of errors concerning mainly settlements are rows of trees along roads, railways and watercourses or trees and bushes enclosing green urban space that are also often classified as hedgerows. Fig. 8 d) shows an example for Munich and f) an example in the city of Aschaffenburg. This is also true for other metropolitan areas within Bavaria, as the hedgerow coverage in Fig. 5

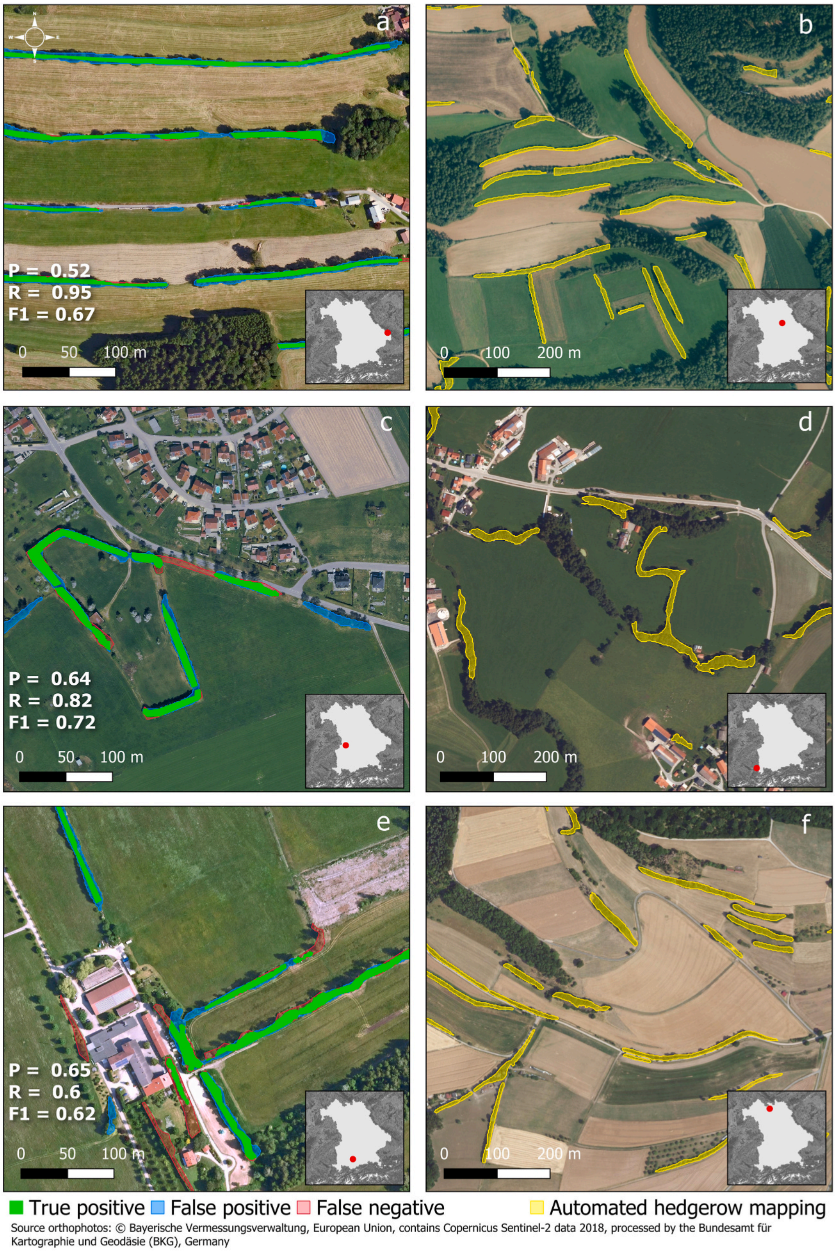

Fig. 7. Results of the automated hedgerow mapping in the test regions a) Freyung-Grafenau, c) Dillingen and e) Weilheim-Schongau divided into true positive (green), false negative (red) and false positive (blue) areas with the original orthophotos at 20 cm resolution. The precision (P), recall (R) and F1-Score (F1) were calculated for the areas visible in each subset. Figures b), d) and f) show examples of the state-wide mapping in the municipalities of Ursensollen, Stiefenhofen and Bad Staffelstein, respectively, where no ground truth data were available.

suggests. The misclassification of hedgerows in urban areas explains the high hedgerow percentages in urban municipalities across Bavaria discussed in section 4.2. Further small errors in our hedgerow dataset may occur on the edges of forest. The model sporadically identifies the first line of trees and shrubs as being a hedgerow (not shown).

4.4. Comparison with other products

4.4.1. Small woody features

The SWF product of the Copernicus HRLs is a new standard product available for delineating SWF in European landscapes. The dataset contains both linear (hedgerows, tree rows etc.) and patchy (i.e. copses, groups of bushes or trees) woody vegetation structures and is delivered at a 5 m resolution (CLMS, 2021). By definition, the SWF product thus comprises more features than our hedgerow

Fig. 8. Typical error types in the automated hedgerow mapping within the test regions with the original orthophotos at 20 cm resolution. True positives are displayed in green, false negatives in red and false positives in blue. The precision (P), recall (R) and F1-Score (F1) were calculated for the areas visible in each subset. Example a) shows undetected hedgerows located in the district of Dillingen. In c), Hassberge, riparian vegetation is erroneously detected by the model and e), Miltenberg, shows misclassifications due to complex cultivation patterns. Other errors found in the Bavaria-wide mapping are the classification of b) riparian vegetation in Straubing, tree rows along alleys and green urban space classified as hedgerows in d) Munich and f) vegetation along railways in Aschaffenburg.

dataset. An in-depth quantitative comparison of the two products was thus not feasible. In the following, we therefore present a mainly descriptive and visual comparison of the SWF 2018 layer with our newly created hedgerow dataset in order to evaluate it.

The SWF dataset includes 1,072,399 polygons across Bavaria which cover 3.37% of the territory, i.e. an area of 2376 km^2. This is 1.9 times the number of polygons in our hedgerow dataset and five times the hedgerow area according to our product (0.67%). Slightly more than half (57%, 272 km^2) of the hedgerow area in our dataset overlaps with polygons of the SWF layer. The median size of the SWFs is 647 m^2 and thus slightly larger as the median size of our hedgerow polygons (594 m^2).

Fig. 9 displays the SWF percentage area per km^2 in Bavaria, in parallel to the illustration of the presented hedgerow map in Fig. 5. Comparing the SWF dataset with our hedgerow map, the two products agree in the overall patterns, but the SWF layer reaches considerably higher values. River networks with riparian vegetation are clearly visible due to their higher SWF coverage. These pixels show values of above 10% up to 20%. High values can also be found in urban areas, particularly in Munich (see subset B). A large amount of woody vegetation in the English Garden, a park area, is included in the SWF layer producing the absolute highest SWF density of 46.3%. Similar to our hedgerow dataset, SWFs are close to absent in the mountainous pre-alpine landscapes in the South and in forested areas. The general gradient of increasing density from South to North and East is, however, not visible in the SWF product.

Compared to the hedgerow coverage at municipality level discussed before (Fig. 6), the spatial patterns are overall similar, but the absolute values reached for SWF coverages are considerably higher. This is described quantitatively in Fig. 10, which compares the distribution of percentage coverages at municipality level for our hedgerows and the SWF. The hedgerow coverage lies for almost all municipalities between 0 and 2% with the median being 0.64%. The SWF, however, cover a much wider percentage range. Most municipalities reach values between 2 and 4%, the median being 3.19%.

Fig. 11 displays some examples of our hedgerow map (yellow) for different locations across Bavaria compared to the polygons of the SWF layer (blue). Our presented approach nicely classified elongated vegetated structures visible on the orthophotos, which were mostly missed by the SWF layer. Fig. 11 a) and b) depict a typical rural, hilly landscape in the municipalities of Oberleichtersbach and Kollnburg where hedgerows mark the boundaries between fields and were classified as such by our automated mapping. The SWF layer, however, only partly describes the elongated structures, but rather maps groups of trees or little copses. This is even more the case in the municipality of Mauth, see Fig. 11 e), where barely any overlap between the two products exists. Higher agreement occurs in the Isar valley close to Gaissach (see Fig. 11 c)). The hedgerows in this region traditionally consist of a mixture of bushes and higher trees. While the extent of the polygons of our automated hedgerow mapping and the SWF showed an overall high agreement, the actual shape of the polygons did not: Based on a visual inspection, the results of our hedgerow dataset followed the shape of the vegetation visible on the orthophoto, shadows are not included and, for most cases, one hedgerow was classified by a single polygon. The SWF polygons are, however, rather irregular and include tree shadows to some extent. Smaller or round shapes are mapped in the SWF layer while they were explicitly not considered in our approach.

In settlements (Fig. 11 d), the SWF layer captures most of the linear structures which were also detected by our model. In addition, also other patchy structures and the larger park in the lower left are classified as SWF. The occurrence of SWF was particularly high in suburban residential areas such as the municipality of Grünwald (Fig. 11 f), where gardens with trees or bushes, common for the area,

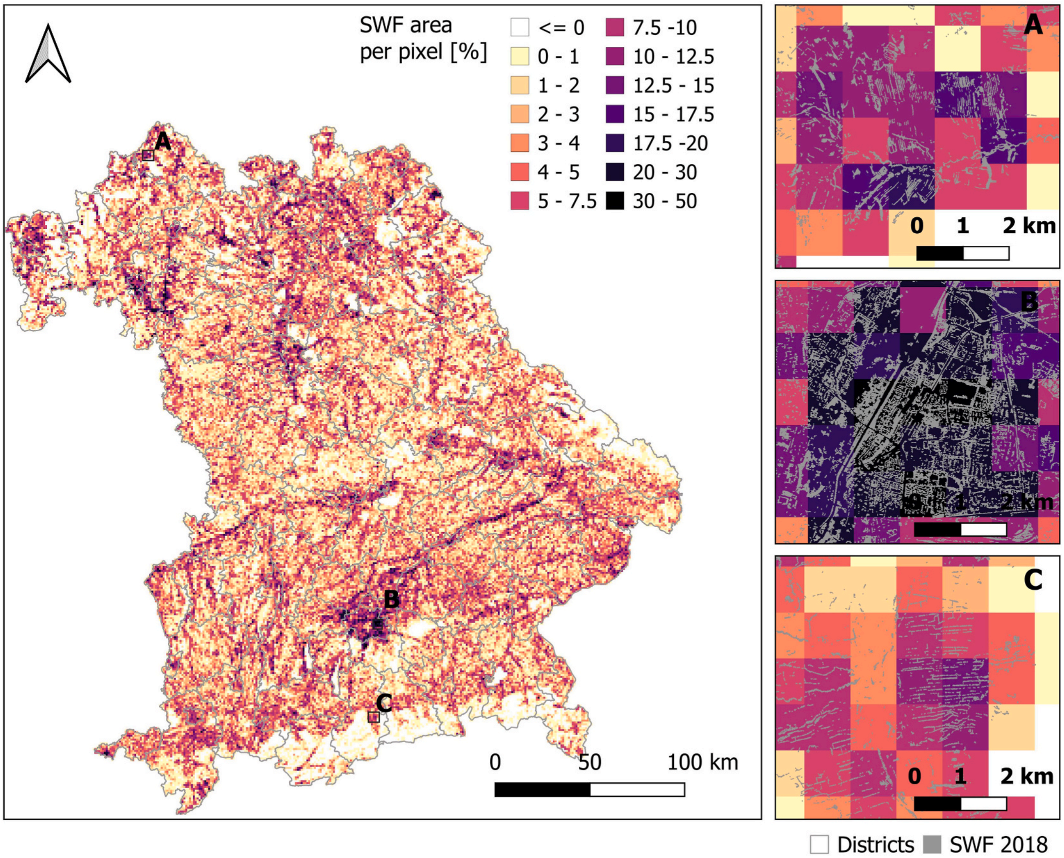

Fig. 9. Small Woody Features (SWF) 2018 area per 1 km × 1 km pixel in percent overlaid by the SWF 2018 polygons (grey) for three close-ups. Subset A shows a close-up of the municipality Bischofsheim in der Rhön, subset B of Munich including the English Garden and subset C the Isar valley at Gaissach.

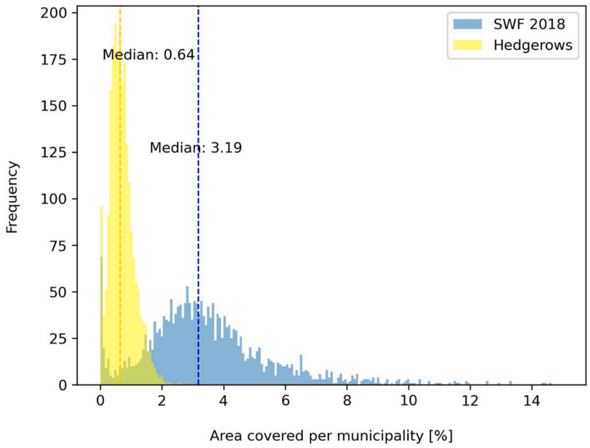

Fig. 10. Distribution of hedgerow (yellow) and SWF percentage coverages (blue) at municipality level.

were largely detected by the SWF layer, but not included in the hedgerow map.

4.4.2. Canopy cover map

The canopy cover map by Liu et al. (2023) is a comprehensive dataset providing information on the location and height of trees (>3m) both within and outside forests. Since the bushes and trees forming hedgerows often – but not always - grow taller than 3 m, we compared this dataset to our hedgerow map (see Fig. 12). For this comparison, we focused solely on the presence or absence of trees outside forests relative to our hedgerows, as our dataset does not include height information.

Overall, the two datasets show a high level of agreement upon visual inspection. However, there are instances where discrepancies arise. For example, as shown in Fig. 12 b), some hedgerows or portions of hedgerows are not captured by the canopy cover map. This omission primarily occurs with narrow hedgerows or those where the vegetation appears to be relatively short, as evidenced in the orthophoto in Fig. 12 a). Conversely, the canopy cover map sometimes includes linear vegetation structures that are not detected by our CNN, as illustrated in Fig. 12 d). These cases often involve wider structures, such as those visible along the eastern border of the subset.

The example in Fig. 12 d) highlights both the strong agreement between the datasets and their primary differences. While the canopy cover map by Liu et al. (2023) captures all visible woody vegetation structures in the orthophoto (Fig. 12 c), our hedgerow map specifically targets narrow, elongated vegetation features. Additionally, the shape of our hedgerow polygons is more precise in some instances, such as those along the road in Fig. 12 d), due to the higher resolution of the input data. Another notable difference is in how hedgerows are represented: in our hedgerow map, individual hedgerows are generally represented by a single polygon, whereas the pixel-based canopy map may omit sections of hedgerows if they are < 3m in height.

5. Discussion

5.1. Hedgerow mapping accuracy

Our study presents the first broad-scale hedgerow mapping approach for an entire state in Germany. With our automated approach using deep learning we were able to detect hedgerows and hedgerow-like structures based on high-resolution orthophotos for a large area. Our map captured hedgerows over a restricted time period of 2–3 years, a great advantage compared to the regular field-assessment that takes place every 20–30 years for a district. It provides valuable information for a range of applications, e.g. to highlight regional differences in hedgerow density within Bavaria.

Our presented CNN-based approach reached only moderate accuracies, e.g. with an F1-Score of 0.48 at pixel level for mapping hedgerows in the five focus districts of Bavaria. The classification accuracies in Table 2 for each single focus district show that there were considerable differences in the model performance depending on the landscape characteristics of the considered region. The F1-Score was generally higher in districts with a high hedgerow percentage such as Freyung-Grafenau or Hassberge. High hedgerow percentages were also found in the district of Miltenberg, for which the lowest F1-score of all districts was achieved. However, many other shrubby or woody biotope types exist in this area according to LfU's biotope dataset, see Table 1. Besides, the mixed use of land as orchards and meadows is characteristic for this district and the landscape in general is very small-structured. These characteristics seem to hamper the accurate and exclusive detection of hedgerows by means of deep learning in this area, as misclassification occurs to a higher extent, resulting in a particularly low precision. Including more training data from such highly complex landscapes could be tested in future studies, once more up-to-date biotope mapping data is available.

The moderate accuracies however do not reflect the good quality of the results that was noticed through visual inspection (section 4.2). Several factors may have negatively affected the presented validation results. A first one is the shape mismatch of the ground truth hedgerow polygons and the detected results: While the hedgerow polygons detected in this study followed the shape of each bush and

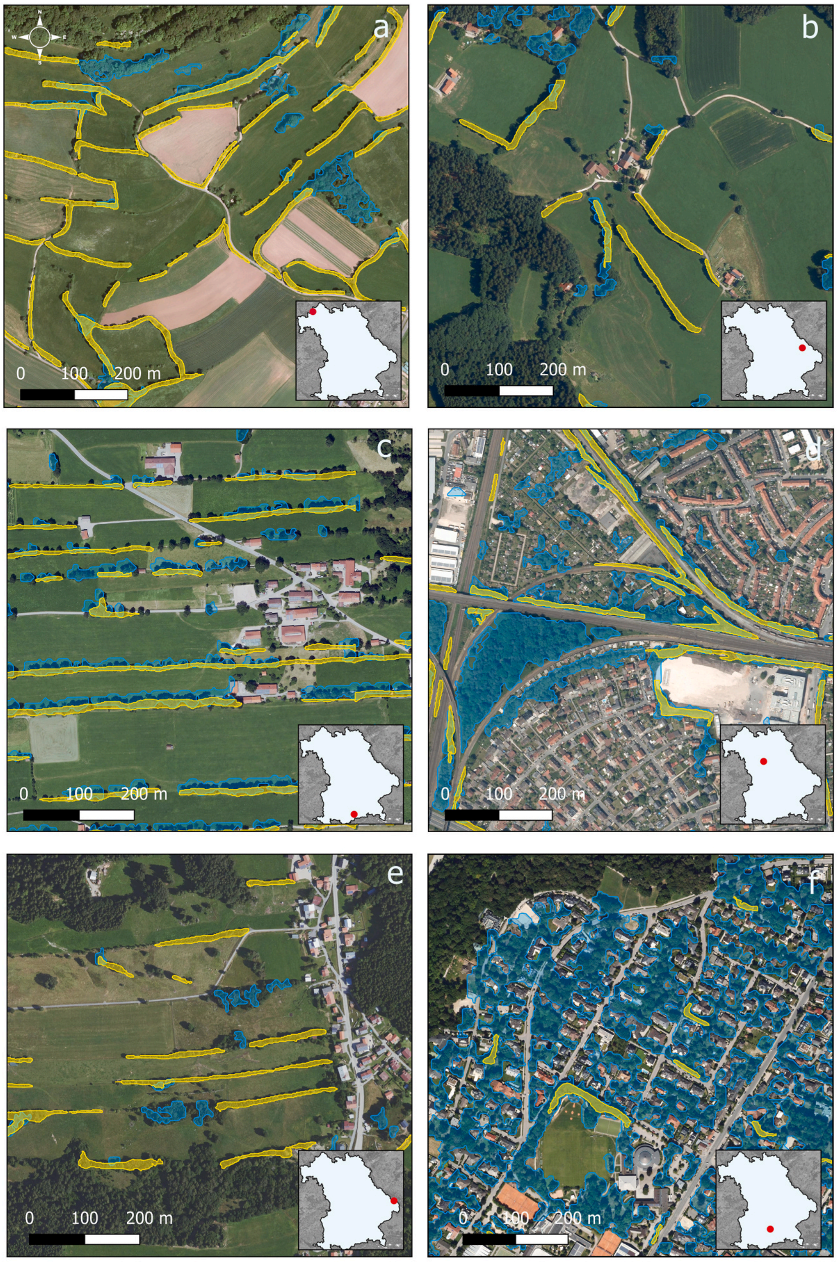

Source orthophotos: © Bayerische Vermessungsverwaltung, European Union, contains Copernicus Sentinel-2 data 2018, processed by the Bundesamt für Kartographie und Geodäsie (BKG), Germany

Fig. 11. Comparison of the automated hedgerow mapping for different locations in Bavaria and the Copernicus Small Woody Features (SWF) Layer. In the municipality of a) Oberleichtersbach and b) Kollnburg hedgerows in an agricultural landscape are accurately mapped by the trained CNN. The SWF Layer misses parts of it, including more copses in turn. In c) Gaissach elongated tree structures are well depicted in both products. In d) Nuremberg urban tree rows are present in both products. In e) Mauth the automated hedgerow mapping and SWF product are very complementary. Vegetation in private gardens in f) Grünwald is included in the SWF Layer.

tree crown, the ground truth hedgerow polygons were digitalized manually and hence showed relatively simple polygon shapes compared to the actual hedgerow shape. In addition, the ground truth polygons originating from the biotope mapping delineate the basis of the hedgerow (the area around the stems) and not the crown by definition (Bayerisches Landesamt für Umwelt, 2022b). Hence, creating the reference dataset was challenging and both in-situ data as well as polygons obtained from visual interpretation had their limitations (Kattenborn et al., 2021). By this means, and particularly due to the conceptual difference between the in-situ reference data (contour of stems) and EO-derived data (contour of crowns), the overlapping area between ground truth and classified hedgerow polygons was reduced.

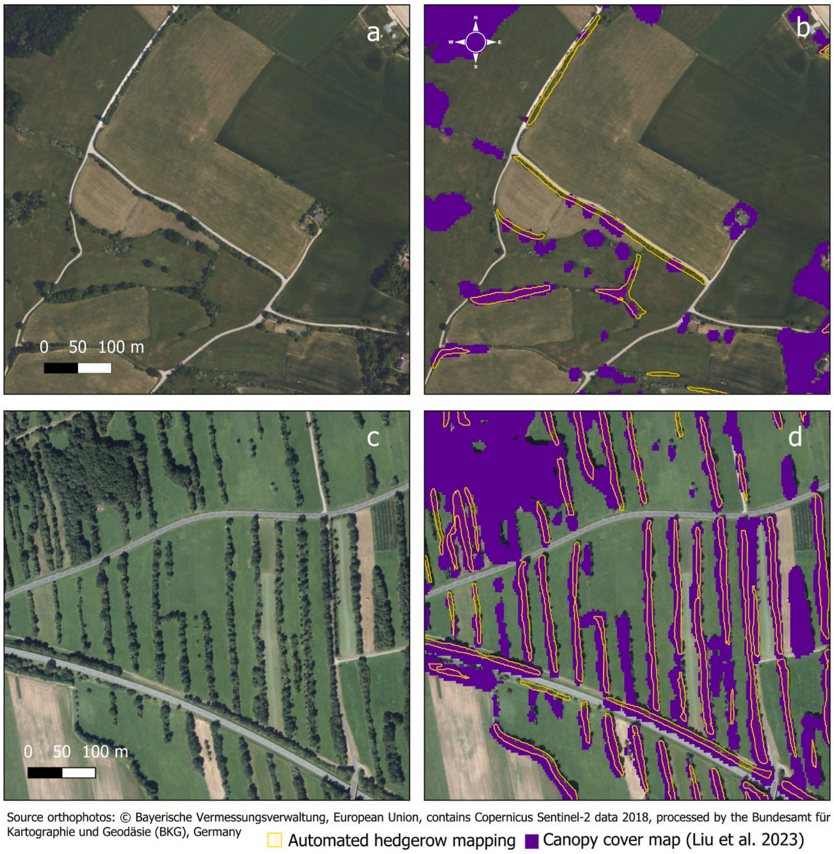

Fig. 12. Comparison of our automated hedgerow mapping and the canopy cover map from Liu et al. (2023) at a location North of Regensburg (a and b) and Bichofsheim in der Rhön (c and d). In a) and c), only the orthophotos are displayed, in b) and d) they are overlayed with the two datasets.

Another important reason for low quantitative accuracy values is the shape and size of the hedgerows. Due to the elongated and narrow shape of hedgerows, even small under- or overestimations of the widths of a hedgerow by only few pixels result in rather high quantitative discrepancies even in cases of seemingly good hedgerow detections (see Fig. 7 a), c) and e)). This issue of optimizing as well as evaluating object detection models for small objects is well known (Chen et al., 2022; Tong et al., 2020; Wei et al., 2024) and becomes also clear in the examples in Figs. 7 and 8. While the results seem to fulfil our expectations from visual inspection, the accuracies are not as high as we expected.

Another reason for differences between our state-wide accuracy results and results of the local study by Ahlswede et al. (2021) might be that they trained a model exclusively for the district of Freyung-Grafenau allowing a higher and specific fit to this relatively homogeneous area. Our model was trained on various landscape structures comprised in rather heterogeneous five focus districts. Although we explicitly selected the mentioned five focus districts to cover different landscape characteristics of Bavaria, we may have missed the whole diversity range. As a consequence, mapping such a large area with a higher variety of landscape types by training a single CNN model is likely to come at the cost of lower F1-Scores. It was, however, the aim of the study to establish a single approach applicable to the entire State of Bavaria, in order to increase the user uptake in public authorities. For future studies, even more emphasize needs to be put on the selection of training data.

Our goal was to focus exclusively on hedgerows and hedgerow-like structures, which is an ambitious task. Hedgerows are very similar to other linear woody vegetation elements, both in terms of spectral characteristics and shape. Other publications considering all kind of "woody vegetation landscape features" (Strnad et al., 2023), "trees outside forests" (Liu et al., 2023), "plant species and communities" (Kattenborn et al., 2019) or "woody vegetation extent" (Flood et al., 2019) achieve higher evaluation metrics. However, these studies do not further subdivide or exclusively map linear features as it is the case for the present study. Indeed, our results (Fig. 7) show that patchy woody vegetation was accurately excluded from the predictions. Our model also successfully excluded forests, even though a forest mask was not applied like in other publications (see e.g. Strnad et al., 2023). It further does not detect linear vegetation structures exceeding a certain width, but solely narrow features that are of a similar width as the training data. Tree and bush rows along roads, railways and watercourses, which where not added to the training and validation set, were still falsely detected as hedgerows by our model due to their geometric resemblance. Since the detection of such structures may be of use for various other applications, see section 5.4, and easily filtered depending on the specific use case, we decided to keep them in our dataset. For the future we plan to include further biotope classes in the model training such as riparian vegetation.

Strnad et al. (2023) found a “notable drop in performance” when applying the same model to images acquired in different years as they “distinct seasonal characteristics”. In our assessment, we did not find any influence of the seasonality on the modelling accuracy using our trained CNN model. This is beneficial given the fact that the Federal State of Bavaria is usually mapped over a two-year period bit by bit during spring, summer and autumn season. However, in future studies, the transferability to orthophotos from other years could be tested, considering the influence of acquisition timing.

5.2. Bavaria-wide Hedgerow map

All in all, the Bavaria-wide results in Fig. 5 show a very plausible distribution of hedgerows across Bavaria reflecting the high landscape variability well. Including the higher density in urban areas caused by the detection of urban linear woody features as mentioned above, the hedgerow distribution is in fact highly variable. It is influenced by factors such as the steepness, topography, geology and the size and shape of agricultural fields which differs depending also on historical-cultural reasons (Reif et al., 1982). The vast, mainly flat southern part of the Danube basin reaching from the north of Munich to the Danube river is intensely used for agriculture, mainly cropland. Hedgerows, and biotopes in general, are rare. This agrees with the data for the focus district Dillingen located in this region, which show that only 2% of this district’s area are biotopes, out of which 5% are natural hedgerows (see Table 1). The Alpine foreland south of Munich, represented by the focus district Weilheim-Schongau, is dominated by grassland farming. Even if it presents a high biotope percentage, hedgerows are not as common as in northern or eastern Bavaria. Meanwhile, the varying topography in northern and eastern Bavaria led to small field sizes. Hedgerows are commonly used for delineating fields and to prevent soil erosion. In fact, the hedgerow percentage for Hassberge (northern Bavaria), and Freyung-Grafenau (eastern Bavaria), are high (see Table 1). This is well reflected in our Bavaria-wide hedgerow mapping.

5.3. Comparison with other products

The SWF layer and our hedgerow dataset differed greatly in their extent, which we expected because the two datasets apply different definitions. The SWF layer includes all kind of woody vegetation, both patchy and linear structures (CLMS, 2021). In our modelling approach, we explicitly excluded patchy structures and focused only on linear ones. Hence, the total area of SWF across Bavaria is five times as large as our total hedgerow area. Still, only 57% of our hedgerows are also present in the SWF layer. This is due to the fact that the SWF layer often misses linear woody vegetation mapped by our model. This clear difference is most likely related to the spatial resolution of the underlying EO data used to derive the features. While the SWF and also the canopy cover map by Liu et al. (2023) rely on spaceborne data at a 2–4 m resolution, we used orthophotos at a 20 cm resolution which allow to detect also narrow hedgerows. The higher resolution of our input data allows our model to clearly delineate features along the edges of the vegetation visible on the orthophoto. In addition, our hedgerows are for the largest part mapped as a single continuous polygon, while in the SWF dataset a single vegetation structure is often represented by several polygons, which is disadvantageous when the number of individual hedgerows is of interest. As for the canopy cover map, it uses a pixel-based approach which does not allow for further analyses on hedgerow geometry or statistical analyses like counting of hedgerows. The exact and continuous mapping of hedgerow polygons in our dataset is an advantage of the higher spatial resolution and object-based approach we used in this study compared to space-borne approaches (CLMS, 2021; Frank et al., 2024; Liu et al., 2023) and may make a great difference when single features need to be analysed. The canopy cover map is a very comprehensive dataset of tall vegetation also outside forests. However, it focuses explicitly on trees and excludes every element below 3 m height. Since this threshold partly omits hedgerows, it is not reliable as sole data source for hedgerow detection.

In summary, we would state that the SWF layer, the canopy cover map and our hedgerow mapping are not redundant, but rather complementary. Our dataset adds many linear features missed in the SWF layer. In combination they can be used to capture the entirety of woody landscape elements outside forests. As for the canopy cover map from Liu et al. (2023), it provides a further dimension by providing also the height of the canopy for all structures higher than 3 m. A combined dataset is certainly of interest for various applications such as the estimation of biomass and carbon storage (Liu et al., 2023), the assessment of the landscape diversity (Musavi et al., 2024; Rubio-Delgado et al., 2024), or habitat connectivity analyses (Bakó et al., 2021; Frank et al., 2024).

5.4. Usage and limitation of hedgerow detection for biotope mapping and other biotope-related applications

The motivation behind generating the presented hedgerow map was to support regular biotope mapping and biotope-related analyses. As shown above, the EO-derived hedgerow map of Bavaria contains, next to the biotope-relevant natural hedgerows, also other linear woody structures, and – though to a lower degree - some natural hedgerows are missed in the map. Because of these limitations, the EO derived map cannot substitute field campaigns that in addition collect data on species composition and other characteristics. Biologists assessing hedgerows in the field and gathering data on the ecological quality of hedgerows on-site are invaluable and indispensable. Still, EO derived maps have great potential to support the in-situ biotope mapping of hedgerows, and particularly the campaign planning.

First, the dataset can be used as calculation basis for estimating the area to be assessed and the costs of mapping campaigns to specify the invitation to tender for subcontractors. In addition, taking an automatically derived hedgerow map to the field, for example on a digital device, could also speed up the mapping process. In this case, the hedgerow polygons do not need to be drawn or updated manually, but just their status has to be checked for changes. This could eventually also reduce the costs of in-situ campaigns. Further, the presented approach has the potential to support more frequent mapping updates, based on the recurring state-wide coverage of aerial imagery that is available every 2–3 years. The results show that the model correctly omits hedgerows that were coppiced or removed, an ability which is essential for monitoring changes over time. Regular mapping updates based on EO could support the identification of hotspots of change, and could thus guide a more focused, punctual in-situ mapping in hotspot regions.

A potential further development of the presented hedgerow map could be to add additional information to each detected polygon. By intersecting our hedgerow map with other geo datasets e.g. on road networks, watercourses, protected areas or agriculture, attributes on location, distance, height or species can be attached. Hence, depending on the user requirements, non-relevant vegetation objects e.g. in urban areas, close to infrastructure, distant from agricultural fields etc., can be filtered out or buffered.

But also beyond biotope mapping, the detection of all kind of linear woody vegetation regardless of its biotope status can be of further value to environmental agencies and scientists. Woody structures like rows of trees and bushes may not cover all ecological aspects of natural hedgerows. Still, they provide shelter as well as food and migration corridors to various species, or they act as windbreaks and sunshade to reduce erosion and evaporation. Apart from the biotope conservation, there are also other protection and funding schemes where such a dataset could provide valuable information focusing for example on biotope networks, landscape elements or regional landscape structure planning (Bayerisches Staatsministerium für Ernährung, 2023; Bayerisches Staatsministerium für Umwelt und Verbraucherschutz, 2022; Bundesamt für Naturschutz, 2024). It further may facilitate the regular reporting of federal environmental agencies on statistical metrics such as hedgerow loss rate and landscape heterogeneity.

Lately, there has been growing interest on the carbon storage potential of hedgerows both in the vegetation biomass as well as in the soil (Biffi et al. 2022, 2023; Tresise et al., 2021). As an example, France introduced a hedgerow management and certification project to enhance the carbon capture capacity of hedgerows (Association Française Arbres Champêtres et Agroforesteries, 2024; ENRD, 2022) and also other countries like Belgium are encouraging the planting of hedgerows (SPW, 2022). A report on the tree cover outside woodland including hedgerows in Great Britain showed, however, that the area covered by these structures may be highly underestimated in some areas (National Forest Inventory, 2017). This illustrates the importance of a detailed hedgerow inventory in the context of carbon accounting.

6. Conclusion

The mapping of hedgerows in the field is very time and resource consuming. Therefore, environmental agencies in Germany such as the Bavarian Environment Agency repeat their in-situ campaigns for each district only every 20–30 years. An up-to-date hedgerow map for the whole of Bavaria, such as the one we created, allows to timely monitor and compare the situation simultaneously across the whole state and to support the large-scale mapping of hedgerows and related environmental analyses by means of remote sensing.

Our final dataset can support field campaigns with additional information on hedgerow distribution and future monitoring. It is best used with other important environmental and administrative variables to maintain more accurate information on a local level. Our map further provides the opportunity to facilitate the campaign planning and speed up the mapping process. Although the dataset includes other linear woody vegetation such as vegetation along watercourses or infrastructure as well, further post-processing, e.g., buffering watercourses, infrastructure, or agricultural fields, allows to add interesting attributes to the dataset or to filter out polygons, depending on the application. These narrow vegetation structures can be of interest for other ecological applications such as heterogeneity analysis and are largely absent in the SWF layer. Hence, our hedgerow map constitutes an important add-on product to the SWF layer including information not available until now for Bavaria. The object-based approach allows to carry out analyses at the level of single features as compared to the canopy cover map. Analyses for diverse purposes such as biomass, carbon storage, habitat connectivity, or biodiversity can be carried out by using our hedgerow map, especially in combination with the SWF layer and canopy cover map including the height information. It has further great potential to support also administrative, nature protection and statistical applications.

CRediT authorship contribution statement

Verena Huber-García: Writing – review & editing, Writing – original draft, Visualization, Formal analysis. **Jennifer Kriese:** Writing – original draft, Validation, Software, Methodology, Investigation. **Sarah Asam:** Writing – review & editing, Writing – original draft, Methodology, Conceptualization. **Mariel Dirscherl:** Software. **Michael Stellmach:** Writing – review & editing, Conceptualization. **Johanna Buchner:** Writing – review & editing, Conceptualization. **Kristel Kerler:** Conceptualization. **Ursula Gessner:** Writing – review & editing, Supervision, Conceptualization.

Ethical Statement

Hereby, I, Verena Huber García, consciously assure that for the manuscript “Hedgerow Map of Bavaria, Germany, based on Orthophotos and Convolutional Neural Networks” the following is fulfilled.

1) This material is the authors’ own original work, which has not been previously published elsewhere.
2) The paper is not currently being considered for publication elsewhere.
3) The paper reflects the authors’ own research and analysis in a truthful and complete manner.
4) The paper properly credits the meaningful contributions of co-authors and co-researchers.
5) The results are appropriately placed in the context of prior and existing research.

6) All sources used are properly disclosed (correct citation). Literally copying of text must be indicated as such by using quotation marks and giving proper reference.

Funding

Agreement on Copernicus User Uptake under grant agreement No. FPA 275/G/GRO/COPE/17/10042, project FPCUP (Framework Partnership Agreement on Copernicus User Uptake), Action 2019-1-6 “Downstream service/application development for monitoring of environmental indicators”.

Declaration of competing interest

The authors declare that they have no known competing financial interests or personal relationships that could have appeared to influence the work reported in this paper.

Acknowledgements

This research was funded by the European Commission’s Caroline Herschel Framework Partnership Agreement. This publication has been prepared using European Union’s Copernicus Land Monitoring Service information, https://doi.org/10.2909/7fd9d32e-8c2f-42b2-b959-c8e12b843821.

LfU provided data on Biotope mapping (© Bayerisches Landesamt für Umwelt) and orthophotos (© Bayerische Vermessungsverwaltung).

We thank Siyu Liu from the Department of Geosciences and Natural Resource Management of the University of Copenhagen, Denmark, for providing the canopy cover & height data at a 3 m resolution for comparison. We also would like to the thank the two anonymous reviewers for their valuable comments.

Data availability

The authors do not have permission to share the original input data. The final hedgerow map of Bavaria will be published soon on the EOC Geoservice of the DLR: https://geoservice.dlr.de/web/.

References

Ahlswede, S., Asam, S., Röder, A., 2021. Hedgerow object detection in very high-resolution satellite images using convolutional neural networks. J. Appl. Rem. Sens. 15, 28. https://doi.org/10.1117/1.JRS.15.018501.

Aksoy, S., Gökhan Akcay, H., Wassenaar, T., 2010. Automatic mapping of linear woody vegetation features in agricultural landscapes using very high resolution imagery. IEEE Trans. Geosci. Remote Sens. 48, 511–522. https://doi.org/10.1109/TGRS.2009.2027702.

Arias, M., Inglada, J., Lucas, R., Blonda, P., 2013. Hedgerow segmentation on VHR optical satellite images for habitat monitoring. Int. Geosci. Remote Sens. Symp. (IGARSS) 3301–3304. https://doi.org/10.1109/IGARSS.2013.6723533. Melbourne, VIC, Australia.

Association Française Arbres Champêtres et Agroforesteries, 2024. La Label Haie: Un label pour préserver les haies. https://labelhaie.fr/. (Accessed 13 December 2024).

Bakó, G., Molnár, Z., Bakk, L., Horváth, F., Fehér, L., Ábrám, Ö., Morvai, E., Biro, C., Pápay, G., Fűrész, A., Penksza, K., Pácsonyi, D., Demény, K., Juhász, E., Dékány, D., Csernyava, L., Illés, G., Molnár, A., 2021. Toward a high spatial resolution aerial monitoring network for nature conservation—how can remote sensing Help protect natural areas? Sustainability 13. https://doi.org/10.3390/su13168807.

Batáry, P., Matthiesen, T., Tscharntke, T., 2010. Landscape-moderated importance of hedges in conserving farmland bird diversity of organic vs. conventional croplands and grasslands. Biol. Conserv. 143, 2020–2027. https://doi.org/10.1016/j.biocon.2010.05.005.

Baudry, J., Bunce, R.G.H., Burel, F., 2000. Hedgerows: an international perspective on their origin, function and management. J. Environ. Manag. 60, 7–22. https://doi.org/10.1006/jema.2000.0358.

Bayerisches Landesamt für Statistik, 2023a. Bodennutzung der landwirtschaftlichen Betriebe in Bayern 2022, Stichprobenerhebung. Fürth, Germany.

Bayerisches Landesamt für Statistik, 2023b. *Flächenerhebung nach Art der tatsächlichen Nutzung in Bayern zum Stichtag 31. Dezember 2022*. Fürth, Germany: Bayerisches Landesamt für Statistik.

Bayerisches Landesamt für Umwelt (LfU), 2022a. Kartieranleitung Biotopkartierung Bayern (inkl. Kartierung der Offenland-Lebensraumtypen der Fauna-Flora-Habitat-Richtlinie) - Teil 1 - Arbeitsmethodik. Augsburg.

Bayerisches Landesamt für Umwelt (LfU), 2022b. Kartieranleitung Biotopkartierung Bayern (inkl. Kartierung der Offenland-Lebensraumtypen der Fauna-Flora-Habitat-Richtlinie) - Teil 2 - Biotoptypen. Augsburg.

Bayerisches Landesamt für Umwelt (LfU), 2022c. Mehr Lebensraum für das Graue Langohr - Ein Leitfaden zur Flurbereicherung.

Bayerisches Landesamt für Umwelt (LfU), 2024. Auswertungen der Kartierungsergebnisse. https://www.lfu.bayern.de/natur/biotopkartierung/auswertung/index.htm.

Bayerisches Staatsministerium für Ernährung, 2023. Landwirtschaft, Forsten und Tourismus. Agrarumwelt- und Klimamaßnahmen (AUKM). https://www.stmelf.bayern.de/foerderung/foerderung-von-agrarumweltmassnahmen-in-bayern/index.html. (Accessed 2 February 2024).

Bayerisches Staatsministerium für Umwelt und Verbraucherschutz, 2022. Biotopverbund in Bayern. Dritter Statusbericht – Berichtsjahr 2022. https://www.naturvielfalt.bayern.de/arten_und_lebensraeume/biotopverbund/doc/statusbericht_2022.pdf.

Betbeder, J., Hubert-Moy, L., Burel, F., Corgne, S., Baudry, J., 2015. Assessing ecological habitat structure from local to landscape scales using synthetic aperture radar. Ecol. Indic. 52, 13. https://doi.org/10.1016/j.ecolind.2014.11.009.

Betbeder, J., Nabucet, J., Pottier, E., Baudry, J., Corgne, S., Hubert-Moy, L., 2014. Detection and characterization of hedgerows using TerraSAR-X imagery. Remote Sens 6, 3752–3769. https://doi.org/10.3390/rs6053752.

Biffi, S., Chapman, P.J., Grayson, R.P., Ziv, G., 2022. Soil carbon sequestration potential of planting hedgerows in agricultural landscapes. J. Environ. Manag. 307, 114484. https://doi.org/10.1016/j.jenvman.2022.114484.

Biffi, S., Chapman, P.J., Grayson, R.P., Ziv, G., 2023. Planting hedgerows: biomass carbon sequestration and contribution towards net-zero targets. Sci. Total Environ. 892, 164482. https://doi.org/10.1016/j.scitotenv.2023.164482.

Boissinot, A., Besnard, A., Lourdais, O., 2019. Amphibian diversity in farmlands: combined influences of breeding-site and landscape attributes in western France. Agric. Ecosyst. Environ. 269, 51–61. https://doi.org/10.1016/j.agee.2018.09.016.

Brandt, M., Tucker, C.J., Kariryaa, A., Rasmussen, K., Abel, C., Small, J., Chave, J., Rasmussen, L.V., Hiernaux, P., Diouf, A.A., Kergoat, L., Mertz, O., Igel, C., Gieseke, F., Schöning, J., Li, S., Melocik, K., Meyer, J., Sinno, S., Romero, E., Glennie, E., Montagu, A., Dendoncker, M., Fensholt, R., 2020. An unexpectedly large count of trees in the West African Sahara and Sahel. Nature 587, 78–82. https://doi.org/10.1038/s41586-020-2824-5.

Broughton, R.K., Burkmar, R., McCracken, M., Mitschunas, N., Norton, L.R., Pallett, D.W., Patton, J., Redhead, J.W., Staley, J.T., Wood, C.M., Pywell, R.F., 2024. UKCEH land cover Plus: hedgerows 2016-2021 (England). https://doi.org/10.5285/d90a3733-2949-4dfa-8ac2-a88aef8699be.

Bundesamt für Naturschutz, 2024. Landschaftsplanung: Ziele, Aufgaben und Inhalte. https://www.bfn.de/landschaftsplanung-ziele-aufgaben-und-inhalte. (Accessed 13 December 2024).

Burke, M.W.V., Rundquist, B.C., Zheng, H., 2019. Detection of shelterbelt density changes using historic APFO and NAIP aerial imagery. Remote Sens 11, 218. https://doi.org/10.3390/rs11030218.

Chen, G., Wang, H., Chen, K., Li, Z., Song, Z., Liu, Y., Chen, W., Knoll, A., 2022. A survey of the four Pillars for small object detection: multiscale Representation, Contextual information, Super-resolution, and region Proposal. IEEE Transactions on Systems, Man, and Cybernetics: Systems 52, 936–953. https://doi.org/10.1109/TSMC.2020.3005231.

Chen, L.-C., Papandreou, G., Schroff, F., Adam, H., 2017. Rethinking atrous convolution for Semantic image segmentation. arXiv preprint. https://arxiv.org/pdf/1706.05587.pdf.

Copernicus Land Monitoring Service, 2019. Small woody features. https://doi.org/10.2909/4e92b07d-48b0-4a53-9db2-fd8d07070cc1.

Copernicus Land Monitoring Service, 2020. CORINE land cover 2018, Version 20.01. https://sdi.eea.europa.eu/catalogue/copernicus/api/records/960998c1-1870-4e82-8051-6485205ebbac?language=all.

Copernicus Land Monitoring Service, 2021. Small Woody Features 2018 and Small Woody Feautures Changes 2015-2018 - User Manual.

Copernicus Land Monitoring Service, 2023. Small woody features. https://doi.org/10.2909/7fd9d32e-8c2f-42b2-b959-c8e12b843821.

Dainese, M., Montecchiari, S., Sitzia, T., Sigura, M., Marini, L., 2017. High cover of hedgerows in the landscape supports multiple ecosystem services in Mediterranean cereal fields. J. Appl. Ecol. 54, 380–388. https://doi.org/10.1111/1365-2664.12747.

Deng, R., Guo, Q., Jia, M., Wu, Y., Zhou, Q., Xu, Z., 2023. Extraction of farmland shelterbelts from remote sensing imagery based on a belt-oriented method. Front. For. Glob. Change 6. https://doi.org/10.3389/ffgc.2023.1247032.

Deng, R.X., Li, Y., Wang, W.J., Zhang, S.W., 2013. Recognition of shelterbelt continuity using remote sensing and waveform recognition. Agrofor. Syst. 87, 827–834. https://doi.org/10.1007/s10457-013-9599-8.

Deng, R.X., Li, Y., Xu, X.L., Wang, W.J., Wei, Y.C., 2016. Remote estimation of shelterbelt width from SPOT5 imagery. Agrofor. Syst. 91, 161–172. https://doi.org/10.1007/s10457-016-9915-1.

Digra, M., Dhir, R., Sharma, N., 2022. Land use land cover classification of remote sensing images based on the deep learning approaches: a statistical analysis and review. Arab. J. Geosci. 15. https://doi.org/10.1007/s12517-022-10246-8.

Dirscherl, M., Dietz, A.J., Kneisel, C., Kuenzer, C., 2021. A Novel method for automated Supraglacial lake mapping in Antarctica using Sentinel-1 SAR imagery and deep learning. Rem. Sens. 1310.3390/rs13020197.

Drexler, S., Gensior, A., Don, A., 2021. Carbon sequestration in hedgerow biomass and soil in the temperate climate zone. Reg. Environ. Change 21, 74. https://doi.org/10.1007/s10113-021-01798-8.

Ducrot, D., Masse, A., Ncibi, A., 2012. Hedgerow detection in HRS and VHRS images from different source (optical, radar). Int. Geosci. Remote Sens. Symp. (IGARSS) 6348–6351. https://doi.org/10.1109/IGARSS.2012.6352712. Munich, Germany.

ENRD, 2022. Enhancing hedgerows' carbon capture capacity. https://ec.europa.eu/enrd/news-events/news/enhancing-hedgerows-carbon-capture-capacity_en.html. (Accessed 13 December 2024).

European Commission, 2020. Communication from the Commission to the European Parliament, the Council, the European Economic and Social Committee and the Committee of the regions on the EU biodiversity strategy for 2030 - Bringing nature back into our lives. https://eur-lex.europa.eu/legal-content/EN/TXT/HTML/?uri=CELEX:52020DC0380&from=EN. (Accessed 15 February 2024).

European Environment Agency, 2023. The Natura 2000 protected areas network. https://www.eea.europa.eu/themes/biodiversity/natura-2000/the-natura-2000-protected-areas-network. (Accessed 15 February 2024).

European Union, 2013. Regulation (EU) No 1306/2013 of the European Parliament and Council of 17 December 2013 on the financing, management and monitoring of the common agricultural policy and repealing Council Regulations (EEC) No 352/78, (EC) No 165/94, (EC) No 2799/98, (EC) No 814/2000, (EC) No 1290/2005 and (EC) No 485/2008. https://eur-lex.europa.eu/legal-content/en/ALL/?uri=CELEX:32013R1306#d1383e1019-549-1. (Accessed 13 May 2024).

Fauvel, M., Planque, C., Sheeren, S., Dalla Mura, M., Cokelaer, F., Chanussov, J., Talbot, H., 2014. Robust path opening versus path opening for the detection of hedgerows in rural landscapes. IEEE Geoscience and Remote Sensing Symposium (IGARSS), pp. 4910–4913. https://doi.org/10.1109/IGARSS.2014.6947596. Quebec City, QC, Canada.

Fauvel, M., Sheeren, D., Chanussot, J., Benediktsson, J.A., 2012. Hedges detection using local directional features and support vector data description. Int. Geosci. Remote Sens. Symp. (IGARSS) 2320–2323. https://doi.org/10.1109/IGARSS.2012.6351030. Munich, Germany.

Flood, N., Watson, F., Collett, L., 2019. Using a U-net convolutional neural network to map woody vegetation extent from high resolution satellite imagery across Queensland, Australia. Int. J. Appl. Earth Obs. Geoinf. 82. https://doi.org/10.1016/j.jag.2019.101897.

Frank, C., Hertzog, L., Klimek, S., Schwieder, M., Tetteh, G.O., Böhner, H.G.S., Röder, N., Levers, C., Katzenberger, J., Kreft, H., Kamp, J., 2024. Woody semi-natural habitats modulate the effects of field size and functional crop diversity on farmland birds. J. Appl. Ecol. 61, 987–999. https://doi.org/10.1111/1365-2664.14604.

Garratt, M.P.D., Senapathi, D., Coston, D.J., Mortimer, S.R., Potts, S.G., 2017. The benefits of hedgerows for pollinators and natural enemies depends on hedge quality and landscape context. Agric. Ecosyst. Environ. 247, 363–370. https://doi.org/10.1016/j.agee.2017.06.048.

Ghimire, K., Dulin, M.W., Atchison, R.L., Goodin, D.G., Hutchinson, J.M.S., 2014. Identification of windbreaks in Kansas using object-based image analysis, GIS techniques and field survey. Agrofor. Syst. 88, 865–875. https://doi.org/10.1007/s10457-014-9731-4.

Graham, L., Gaulton, R., Gerard, F., Staley, J.T., 2018. The influence of hedgerow structural condition on wildlife habitat provision in farmed landscapes. Biol. Conserv. 220, 122–131. https://doi.org/10.1016/j.biocon.2018.02.017.

He, K., Zhang, X., Ren, S., Sun, J., 2016. Deep residual learning for image recognition. Proceedings of the IEEE Conference on Computer Vision and Pattern Recognition, pp. 770–778.

Hoeser, T., Bachofer, F., Kuenzer, C., 2020. Object detection and image segmentation with deep learning on earth observation data: a review - Part II: applications. Remote Sens 12, 3053. https://doi.org/10.3390/rs12183053.

Holden, J., Grayson, R.P., Berdeni, D., Bird, S., Chapman, P.J., Edmondson, J.L., Firbank, L.G., Helgason, T., Hodson, M.E., Hunt, S.F.P., Jones, D.T., Lappage, M.G., Marshall-Harries, E., Nelson, M., Prendergast-Miller, M., Shaw, H., Wade, R.N., Leake, J.R., 2019. The role of hedgerows in soil functioning within agricultural landscapes. Agric. Ecosyst. Environ. 273, 1–12. https://doi.org/10.1016/j.agee.2018.11.027.

Institut National de l'Information Géoraphique et Forestière (IGN), 2021. BD haies. https://geoservices.ign.fr/bdhaie.

Kattenborn, T., Eichel, J., Fassnacht, F.E., 2019. Convolutional Neural Networks enable efficient, accurate and fine-grained segmentation of plant species and communities from high-resolution UAV imagery. Sci. Rep. 9. https://doi.org/10.1038/s41598-019-53797-9.

Kattenborn, T., Leitloff, J., Schiefer, F., Hinz, S., 2021. Review on convolutional neural networks (CNN) in vegetation remote sensing. ISPRS J. Photogramm. Remote Sens. 173, 24–49. https://doi.org/10.1016/j.isprsjprs.2020.12.010.

Kingma, D.P., Lei Ba, J., 2015. Adam: a method for Stochastic Optimization. 3rd International Conference for Learning Representations 1412, 6980. https://doi.org/10.48550/arXiv.1412.6980. San Diego.

Kriese, J., Hoeser, T., Asam, S., Kacic, P., Da Ponte, E.D., Gessner, U., 2022. Deep learning on synthetic data enables the automatic identification of Deficient forested windbreaks in the Paraguayan Chaco. Rem. Sens. 1410.3390/rs14174327.

Lecq, S., Loisel, A., Brischoux, F., Mullin, S.J., Bonnet, X., 2017. Importance of ground refuges for the biodiversity in agricultural hedgerows. Ecol. Indic. 72, 615–626. https://doi.org/10.1016/j.ecolind.2016.08.032.

Liu, S., Brandt, M., Nord-Larsen, T., Chave, J., Reiner, F., Lang, N., Tong, X., Ciais, P., Igel, C., Pascual, A., Guerra-Hernandez, J., Li, S., Mugabowindekwe, M., Saatchi, S., Yue, Y., Chen, Z., Fensholt, R., 2023. The overlooked contribution of trees outside forests to tree cover and woody biomass across Europe. Sci. Adv. 9, eadh4097. https://doi.org/10.1126/sciadv.adh4097.

Luscombe, D.J., Gatis, N., Anderson, K., Carless, D., Brazier, R.E., 2023. Rapid, repeatable landscape-scale mapping of tree, hedgerow, and woodland habitats (THaW), using airborne LiDAR and spaceborne SAR data. Ecol. Evol. 13, e10103. https://doi.org/10.1002/ece3.10103.

Ma, L., Liu, Y., Zhang, X., Ye, Y., Yin, G., Johnson, B.A., 2019. Deep learning in remote sensing applications: a meta-analysis and review. ISPRS J. Photogramm. Remote Sens. 152, 12. https://doi.org/10.1016/j.isprsjprs.2019.04.015.

Magel, H., 2012. Flurbereinigung. http://www.historisches-lexikon-bayerns.de/Lexikon/Flurbereinigung. (Accessed 15 February 2024).

Maxwell, A.E., Warner, T.A., Guillén, L.A., 2021. Accuracy assessment in convolutional neural network-based deep learning remote sensing studies - part2: Recommendations and best Practices. Remote Sens 13. https://doi.org/10.3390/rs13132450.

McGarigal, K., 2015. Fragstats Help. University of Massachusetts, Amherst, USA.

Montgomery, I., Caruso, T., Reid, N., 2020. Hedgerows as ecosystems: service Delivery, management, and Restoration. Annu. Rev. Ecol. Evol. Syst. 51, 81–102. https://doi.org/10.1146/annurev-ecolsys-012120-100346.

Morandin, L.A., Garbach, K., Long, R.F., 2017. Hedgerow benefits align with food production and sustainability goals. Calif. Agric. 71, 117–119. https://doi.org/10.3733/ca.2017a0020.

Musavi, T., Skøien, J., Czúcz, B., Hagyo, A., Sedano, F., Martinez-sanchez, L., Koeble, R., van der velde, M., Terres, J.-M., D'Andrimont, R.d.A., 2024. Bridging field Surveys and remote sensing for enhanced landscape feature analysis in EU agriculture. In: EGU General Assembly 2024. Vienna, Austria.

National Forest Inventory, 2017. Tree Cover outside Woodland in Great Britain. Forestry Commission, Edinburgh.

O'Connell, J., Bradter, U., Benton, T.G., 2015. Wide-area mapping of small-scale features in agricultural landscapes using airborne remote sensing. ISPRS J. Photogramm. Remote Sens. 109. https://doi.org/10.1016/j.isprsjprs.2015.09.007.

Oquab, M., Bottou, L., Laptev, I., Sivic, J., 2014. Learning and Transferring Mid-level Image Representations Using Convolutional Neural Networks. IEEE Conference on Computer Vision and Pattern Recognition, Columbus, OH, USA, pp. 1717–1724. https://doi.org/10.1109/CVPR.2014.222.

Pelletier-Guittier, C., Théau, J., Dupras, J., 2020. Use of hedgerows by mammals in an intensive agricultural landscape. Agric. Ecosyst. Environ. 302. https://doi.org/10.1016/j.agee.2020.107079.

Piwowar, J.M., Amichev, B.Y., Van Rees, K.C.J., 2016. The Saskatchewan shelterbelt inventory. Can. J. Soil Sci. 97 (3). https://doi.org/10.1139/cjss-2016-0098.

Razafimaharo, C., Krähenmann, S., Höpp, S., Rauthe, M., Deutschländer, T., 2020. New high-resolution gridded dataset of daily mean, minimum, and maximum temperature and relative humidity for Central Europe (HYRAS). Theor. Appl. Climatol. 142, 1531–1553. https://doi.org/10.1007/s00704-020-03388-w.

Reif, A.S., E, D., Zahner, K., 1982. Der Einfluß des geologischen Untergrundes, der Hangneigung, der Feldgröße und der Flurbereinigung auf die Heckendichte in Oberfranken. Ber. ANL 6, 231–253.

Rubio-Delgado, J., Schnabel, S., Lavado-Contador, J.F., Schmutz, U., 2024. Small woody features in agricultural areas: Agroforestry systems of overlooked significance in Europe. Agric. Syst. 218, 103973. https://doi.org/10.1016/j.agsy.2024.103973.

shuaizzZ, 2020. Dice-Loss-PyTorch. in. github.Com.

Smigaj, M., Gaulton, R., 2021. Capturing hedgerow structure and flowering abundance with UAV remote sensing. Remote Sens. Ecol. Conserv. 7, 521–533. https://doi.org/10.1002/rse2.208.

SPW, 2022. Le projet - Yes! We plant. http://yesweplant.wallonie.be/cms/render/live/fr/sites/haies/home/le-projet.html. (Accessed 13 December 2024).

Strnad, D., Horvat, Š., Mongus, D., Ivajnšič, D., Kohek, Š., 2023. Detection and monitoring of woody vegetation landscape features using periodic aerial Photography. Remote Sens 15. https://doi.org/10.3390/rs15112766.

Sun, R., Song, C., Sun, Y., Wang, Q., Liu, H., Wang, J., 2020. Agricultural soil organic Matters and microbiome are shaped by management and hedgerows. Agronomy 10, 1316. https://doi.org/10.3390/agronomy10091316.

Tansey, K., Chambers, I., Anstee, A., Denniss, A., Lamb, A., 2009. Object-oriented classification of very high resolution airborne imagery for the extraction of hedgerows and field margin cover in agricultural areas. Appl. Geogr. 29, 145–157. https://doi.org/10.1016/j.apgeog.2008.08.004.

Tong, K., Wu, Y., Zhou, F., 2020. Recent advances in small object detection based on deep learning: a review. Image Vis Comput. 97, 103910. https://doi.org/10.1016/j.imavis.2020.103910.

Torch Contibutors, 2023. DEEPLABV3_RESNET50. In: pytorch.org.

Tresise, M.E., Reed, M.S., Chapman, P.J., 2021. Effects of hedgerow enhancement as a net zero strategy on farmland biodiversity: a rapid review. Emerald Open Research 1. https://doi.org/10.1108/eor-10-2023-0011.

Tucker, C., Brandt, M., Hiernaux, P., Kariryaa, A., Rasmussen, K., Small, J., Igel, C., Reiner, F., Melocik, K., Meyer, J., Sinno, S., Romero, E., Glennie, E., Fitts, Y., Morin, A., Pinzon, J., McClain, D., Morin, P., Porter, C., Loeffler, S., Kergoat, L., Issoufou, B.-A., Savadogo, P., Wigneron, J.-P., Poulter, B., Ciais, P., Kaufmann, R., Myneni, R., Saatchi, S., Fensholt, R., 2023. Sub-continental-scale carbon stocks of individual trees in African drylands. Nature 615, 80–86. https://doi.org/10.1038/s41586-022-05653-6.

Vali, A., Comai, S., Matteucci, M., 2020. Deep learning for land Use and land cover classification based on Hyperspectral and Multispectral earth observation data: a review. Remote Sens. 12, 2495. https://doi.org/10.3390/rs12152495.

Vannier, C., Hubert-Moy, L., 2008. Detection of wooded hedgerows in high resolution satellite images using an object-oriented method. Int. Geosci. Remote Sens. Symp. (IGARSS) 5, 731–734. https://doi.org/10.1109/IGARSS.2008.4779826. Boston, MA, USA.

Vannier, C., Hubert-Moy, L., 2010. Wooded hedgerows characterization in rural landscape using very high spatial resolution satellite images. Int. Geosci. Remote Sens. Symp. (IGARSS) 347–350. https://doi.org/10.1109/IGARSS.2010.5651636. Honolulu, HI, USA.

Vannier, C., Hubert-Moy, L., 2014. Multiscale comparison of remote-sensing data for linear woody vegetation mapping. Int. J. Remote Sens 35, 7376–7399. https://doi.org/10.1080/01431161.2014.968683.

Visvalingam, M., Whyatt, J.D., 1993. Line generalisation by repeated elimination of the smallest area. J. Cartogr. 30, 46–51. https://doi.org/10.1179/000870493786962263.

Wei, W., Cheng, Y., He, J., Zhu, X., 2024. A review of small object detection based on deep learning. Neural Comput. Appl. 36, 6283–6303. https://doi.org/10.1007/s00521-024-09422-6.

Wolton, R., 2015. Life in a hedge. Br. Wildl. 26, 306–316. https://plantenvanhier.nl/onewebmedia/Robert%20Wolton%20-%20Life%20in%20a%20hedge%20-%20British%20Wildlife%202015.pdf.

Wurm, M., Stark, T., Zhu, X.X., Weigand, M., Taubenböck, H., 2019. Semantic segmentation of slums in satellite images using transfer learning on fully convolutional neural networks. ISPRS J. Photogramm. Remote Sens. 150, 59–69. https://doi.org/10.1016/j.isprsjprs.2019.02.006.

Zhao, R., Qian, B., Zhang, X., Li, Y., Wei, R., Liu, Y., Pan, Y., 2020. Rethinking Dice loss for medical image segmentation. In: IEEE International Conference on Data Mining (ICDM), pp. 851–860. https://doi.org/10.1109/ICDM50108.2020.00094. Sorrento, Italy.

Zhao, S., Tu, K., Ye, S., Tang, H., Hu, Y., Xie, C., 2023. Land Use and land cover classification Meets deep learning: a review. Sensors 23. https://doi.org/10.3390/s23218966.